Apoptosis (2022) 27:90–111
https://doi.org/10.1007/s10495-021-01702-z

Benzofuran pyran hybrid prevents glucocorticoid induced osteoporosis in mice via modulation of canonical Wnt/β-catenin signaling

Ashish Kumar Tripathi[1] · Divya Rai[1,3] · Priyanka Kothari[1] · Pragati Kushwaha[2] · Koneni V. Sashidhara[2] · Ritu Trivedi[1]

Accepted: 29 November 2021 / Published online: 2 February 2022

Abstract

Glucocorticoid induced osteoporosis (GIOP) is the second most leading cause of osteoporosis. We have identified a compound, a benzofuran pyran hybrid compound 4e that has osteogenic potential and we wanted to assess its efficacy in GIOP in male mice. We assessed the effect of dexamethasone and compound 4e on primary osteoblasts using various cell based and immunofluorescence assays. For in vivo studies we administered methylprednisolone and compound 4e as a prophylactic measure in male Balb/c mice for 28 days and then evaluated the effect on bone microarchitecture by microCT, bone formation by histology along with clinically relevant bone markers. Compound 4e preserved osteoblast differentiation as evident by higher ALP positive cells and mineralization in compound treated groups. Compound 4e also increased the expression of osteogenic genes. This compound guarded β-catenin expression both in vitro and in vivo as confirmed by western blot and immunofluorescence assays. This led to the preservation of bone microarchitecture and cortical thickness at 2.5 mg kg^{-1} and 5 mg kg^{-1} doses. Further compound 4e enhanced bone formation rate and regulated osteocyte death. The osteogenic potential of compound 4e was reflected by an increased level of serum marker osteocalcin and decreased levels of SOST and CTX-I. Overall, Compound 4e is able to overcome the catabolic effect of dexamethasone on bone by targeting the canonical WNT/β-catenin signaling as evidenced by both in vitro and in vivo studies.

Keywords Wnt/β-catenin · Glucocorticoid-induced osteoporosis · Osteoblast · Benzofuran pyran

Abbreviations

GIOP	Glucocorticoid-induced osteoporosis
MP	Methylprednisolone
DEX	Dexamethasone
MTT	3-(4,5-Dimethylthiazol-2-yl)-2, 5-Diphenyltetrazolium Bromide
BMD	Bone mineral density
ALP	Alkaline phosphatase
RANK	Receptor activator of nuclear factor kappa-B
RUNX2	Runt-related transcription factor 2
OCN	Osteocalcin
BMP2	Bone morphogenetic protein 2
SOST	Sclerostin

Introduction

Glucocorticoids (GC) are indispensable drugs prescribed by clinicians for various diseases like allergy, rheumatoid arthritis, COPD (chronic obstructive pulmonary disease), SLE (systemic lupus erythematous), inflammatory bowel disease, and other systemic diseases [1]. Approximately 0.5–1% general population is receiving chronic glucocorticoid treatment [2, 3]. Dexamethasone a synthetic glucocorticoid by its anti-inflammatory and immunosuppressive effects has recently shown its benefits and prevented one-third of deaths among Covid-19 patients who were critically ill [4]. However, long-term use of glucocorticoid is associated with fragility of bones and an increased risk of fracture and this is called glucocorticoid-induced osteoporosis (GIOP), the most common form of secondary osteoporosis. The effect

✉ Ritu Trivedi
ritu_trivedi@cdri.res.in; ritu_pgi@yahoo.com

[1] Endocrinology Division, CSIR-Central Drug Research Institute, 10/1, Sector 10, Jankipuram Extension, Sitapur Road, Lucknow, Uttar Pradesh 226031, India

[2] Medicinal and Process Chemistry Division, CSIR-Central Drug Research Institute, Lucknow 226031, India

[3] Academy of Scientific and Innovative Research (AcSIR), Ghaziabad 201002, India

of glucocorticoid on bone is time and dose-dependent. Increased risk of fragility fracture may occur even at the lower dose of glucocorticoid in the first month of treatment [5]. About 30–50% of patients receiving long-term glucocorticoid develop glucocorticoid induced osteoporosis [6]. Initial glucocorticoid intake results in a transient increase in bone resorption as glucocorticoids enhance the production of RANKL (Receptor activator of nuclear factor kappa-B ligand) and diminish OPG (Osteoprotegerin) expression [7, 8]. Glucocorticoids suppress bone formation by maneuvering the primary bone formation pathway WNT/β-catenin signaling [9]. Glucocorticoid induces the expression of Sclerostin (SOST) a Wnt pathway inhibitor thus hampers bone formation [9]. Glucocorticoid also inhibits bone formation by inducing BMP-RUNX2 pathway inhibitors [10]. At physiological concentration, glucocorticoid stimulates mesenchymal stem cells to differentiate into osteoblast lineage rather than adipocyte lineage via suppression of sFRP-1 (Secreted frizzled-related protein 1) but at pharmacological doses, glucocorticoid favors adipocyte lineage by increasing the expression of PPAR-γ which might be the physiological basis behind the accumulation of bone marrow fat accompanying bone loss in patients with long-standing glucocorticoid treatment [11–14]. GC treatment leads to enlarged osteocyte lacunae (osteolysis) and increased autophagy as a defensive mechanism to survive stress whereas overexposure at higher doses leads to apoptosis [15]. Apart from the aforementioned mechanism glucocorticoids also induce osteoblast death by increasing reactive oxygen species (ROS) mediated phosphorylation of JNK and induction of oxidative DNA and anti-oxidative stress defence system damage [16].

To date, bisphosphonates are used as first-line therapy for GIOP, followed by treatment with PTH and Teriparatide. Bisphosphonates are relatively safe drugs but long term usage carries a warning of osteonecrosis of the jaw and atypical femoral fractures [17, 18]. Another treatment includes Denosumab, a monoclonal antibody against RANKL that increases lumber BMD when compared to Risedronate (bisphosphonate) in a randomized double-blind, double-dummy, active-controlled study [19]. A concern with Denosumab treatment in GIOP is a possible increase in vertebral fracture after stopping the drug [20]. Teriparatide can only be prescribed for a maximum of 24 months of treatment in patients with GIOP; however, due to its higher cost and inconvenience of daily subcutaneous injection, its use in GIOP has been limited. Given these side effects and cost burden, there is a need for a potential candidate with lesser or no side effects.

Compound 4e is a member of the benzofuran-pyran hybrid chemical class. Benzofuran scaffolds are believed to be an essential member of heterocyclic compounds and known for various biological activities like anti-hyperglycemic [21]), anti-parasitic [22], antimicrobial [23], antitumor, and kinase inhibitor activities [24]. The effects of benzofuran compounds as anti-osteoporotic agents have been explored many times. Fontana et.al. had shown bone loss inhibitory activity of benzofuran. Likewise, the derivative of benzofuran is known for its anti-resorptive activity by inhibiting Cathepsin K [25]. Our previous studies have shown the bone forming ability of Benzofuran-dihydropyridine hybrids in the drill hole model of fracture [26]. Studies show that Bergapten, a natural product related to benzofuran ring structure enhances the BMP2 activity by modulating the P38 and ERK dependent pathway in osteoblasts [27]. Pyrans were also extensively studied for their osteogenic activities [28, 29]. Observations by us confirm that compound 4e is known for its osteogenic [30] and anti lipotoxic [31] effects. This led us to explore the potential of Benzofuran-dihydropyridine hybrids in glucocorticoid induced osteoporosis.

Materials and methods

In vitro experiments

Primary osteoblast culture

Primary osteoblasts were harvested from 2 to 3 days old mice pups. Briefly, calvaria of pups (n = 6) was surgically removed and cleaned. Each calvaria was chopped into small pieces then exposed in enzymatic solution (1 mg/ml of Collagenase I and Dispase II) for 15 min at 37 °C. First digestion was discarded as it contains more brain parts, fibroblast, and other debris. From second digestion onwards supernatant was collected in 10% complete alpha MEM. Cells were plated in T-25 flask and after reaching 70–80% confluency cells were harvested for further use [31, 32].

MTT assay

Cells were seeded and treated as above mentioned in complete alpha MEM media for 48 h. After the end of the experiment, MTT (5 mg/ml) was added to each well for 2–4 h. After the desired time DMSO was added to dissolve formazan crystal and absorbance was taken at 570 nm [33].

Annexin/Pi apoptosis assay

Osteoblasts were grown in T-25 flask. After achieving 70–80% confluency cells were treated with dexamethasone and compound 4e at 10 nM and 0.1 µM concentration for 48 h. Dead cell apoptosis kit from Invitrogen was used to quantify live and apoptotic cells through flow cytometry. Cells were processed according to the manufacturer's protocol [34].

TUNEL assay

Osteoblasts were grown on a coverslip and treated with dexamethasone and compound 4e. Cells were washed with PBS fixed with paraformaldehyde then permeabilized with 0.25% TritonX-100. After the permeabilization, we used Click-iT™ Plus TUNEL Assay (C10617 Invitrogen) to detect apoptotic cells tagged with alexa fluor 488. To detect apoptosis in tissue we dewaxed and rehydrated bone tissue in Ethanol and water. Then processed according to manufacturer's protocol [33].

Intracellular ROS detection

Cells were grown in 12 and 96 well plates and treated with dexamethasone, compound 4e at the concentration 10 nM and 0.1 µM for 24 h. Osteoblasts cells were washed twice with PBS and then incubated with 5 µM 2′,7′-dichlorofluorescein diacetate (DCFH-DA) for 45 min at 37 °C. Fluorescent images were captured using Evos Fl Fluorescent microscope (Applied Biosystems) at × 10 magnification and absorbance was measured by Spectra max M2 Molecular Devices at 485/535 nm. [35].

Alkaline phosphatase assay and staining

Cells were seeded in 96 well plates at 2×10^3 density. After reaching 70% confluency cells were treated with different concentrations, 10 nM, 0.1 µM, 0.5 µM, and 1 µM, of compound 4e with or without dexamethasone (1 µM) for 48 h in osteogenic media (10 mM β-Glycerophosphate and 50 µg/ml Ascorbic acid in Alpha MEM). After 48 h cells were washed with PBS and kept at − 80 °C for overnight. The next day cells were kept at 37 °C, this quick temperature change burst the cell and expose the ALP enzyme. ALP enzymes were quantified by pNPP (para-Nitrophenyl phosphate), which is a substrate for ALP, by a colorimetric ELISA plate reader at 405 nm. For ALP staining cells were treated as above mentioned. At the end of the experiment, cells were washed with PBS and incubated in 1-Step™ NBT/BCIP Substrate Solution for 30 min and then washed with PBS. Imaging was done with Evos Xl (Applied biosystems) at × 10 magnification. ALP positive cells were quantified with IMAGE Pro software [26, 36].

Mineralized nodule formation assay

Calvarial osteoblasts were seeded in 12 well plates and treatment of compound 4e and dexamethasone were given as mentioned in ALP assay for 21 days. Media were changed after every 48 h. After the end of the experiment, cells were washed with PBS and fixed in 4% formaldehyde for 30 min then incubated in Alizarin Red S stain for another 30 min. Cells were then washed with tap water and PBS. Images of mineralized nodules were captured with Nikon Coolpix B600. For quantification of mineralized nodules, 10% (v/v) acetic acid was added to each well with shaking at room temperature for 30 min. Cells were scraped out and collected in a microcentrifuge tube then centrifuged at 20,000×*g* for 15 min after that supernatant was collected. 10% (v/v) ammonium hydroxide was added to the supernatant to bring the pH of the solution to 4.5 for color formation. The absorbance of the solution was read at 405 nm [37].

Real-time PCR

Primary osteoblasts were treated with dexamethasone and compound 4e as mentioned for ALP assay for 48 h. At the end of the experiment, RNA was isolated by using Quizol (Qiagen) and cDNA was made by High capacity cDNA reverse transcription kit (Thermo Fisher). We performed real-time PCR (Quant Studio 3, Applied Biosystems) for assessment of gene expression by SYBR green (PowerUp SYBR Green master mix Applied Biosystems). We checked gene expression of RUNX2, BMP2, ALP, β-catenin, SOST (Table 1) in response to dexamethasone and compound 4e [33].

Western blot analysis

Primary osteoblasts cells were treated as above mentioned and lysed in buffer containing 1 × RIPA lysis buffer, protease inhibitor, and phosphatase inhibitor. Protein concentration was quantified using a BCA Protein Assay kit (Thermo Fisher Scientific, MA, USA) according to the manufacturer's instructions. Proteins were separated by sodium dodecyl sulfate polyacrylamide gel electrophoresis (SDS-PAGE) and transferred to a poly-vinylidene difluoride membrane (PVDF, Millipore, MA, USA). After blocking with 5% BSA in Tween-20/PBS (PBST) at room temperature for 2 h, membranes were incubated with specific primary antibodies at 4 °C overnight. Thereafter, membranes were probed with HRP-conjugated secondary antibody for 2 h at room temperature and chemiluminescence was detected with an enhanced chemiluminescence system (ECL, MERCK Millipore, MA, USA). Results were normalized to β-actin. [38].

Immunocytochemistry

Cells were grown in 4 well chamber slides. Cells were treated with dexamethasone and compound 4e as above mentioned for 48 h. At the end of the experiment, cells were fixed with 4% formaldehyde and permeabilized with 0.25% Triton × 100. Cells were then blocked with 2% BSA and incubated with RUNX2 antibody (12556 CST, dilution 1:100) overnight at 4^0C. Further RUNX2 antibody probed

Table 1 Primer sequence used for qPCR

Gene symbol	Gene name	Primer sequence	Accession number
BMP-2	Bone morphogenetic protein-2	F-CGGACTGCGGTCTCCTAA R-GGGGAAGCAGCAACACTAGA	NM_007553.2
ALP	Alkaline phosphatase	F-TCATGATGTCCGTGGTCAAT R-CGGATCCTGACCAAAAACC	NM_007431.3
RUNX2	Runt-related transcription factor-2	F-GCCCAGGCGTATTTCAGA R-TGCCTGGCTCTTCTTACTG	NM_001145920.2
SOST	Sclerostin	F-CAGGAGAGGAAGCTTGAGTCC R-AGGGTAGAAAGACCCCCATC	NM_024449.6
RANKL	Receptor activator of nuclear factor kappa-B ligand	F-AGCCATTTGCACACCTCAC R-CGTGGTACCAAGAGGACAGAGT	NM_011613.3
OPG	osteoprotegerin	F-CGAGTGTGTGAGTGTGAGGAA R-ACAGCTCCGGTGCTTCAA	NM_008764.3
β-Cat	β-catenin	F-TTCCTATGGGAACAGTCGAAG R-TTGTATTGTTACTCCTCGACCAAA	NM_001165902.1
GAPDH	Glyceraldehyde 3-phosphate dehydrogenase	F-AGCTTGTCATCAACGGGAAG R-TTTGATGTTAGTGGGGTCTCG	DQ403054.1

with Alexa Fluor 488 (1:200 dilution) and DAPI were used for nuclear stain. β-catenin (SC-7199, dilution 1:100 dilution) was used and Alexa fluor 594 (1:200 dilution) was used as a secondary antibody. Images were taken in Leica confocal microscope at × 40 magnification [31].

In vivo experiments

All animal care and experimental procedures were approved by the Institutional Animal Ethics Committee (IAEC) [approval no. IAEC/2017/44(234/17)] and performed according to the regulations of the Council for the Purpose of Control and Supervision of Experiments on Animals, Ministry of Social Justice and Empowerment, Government of India. 10–12 week old male BALB/c mice (weighing 22 ± 2 g each), were obtained from the National Laboratory Animal Centre, CSIR-CDRI, housed in a 12-h/12-h light/dark cycle with controlled temperature (22–24 °C) and humidity (50–60%). Standard rodent chow diet and water were provided ad libitum. Animals were randomly divided in four groups (n = 10 mice/group), Control, Methylprednisolone (10 mg kg^{-1}), Methylprednisolone + Compound 4e 5 mg kg^{-1} and 10 mg kg^{-1} for 28 days. Methylprednisolone was given subcutaneously and compound 4e was administered orally. To detect dynamic bone formation each animal was given calcein (20 mg kg^{-1}) intraperitoneally 7 days and 1 day before sacrifice.

Microcomputed tomography (μCT)

Micro-computed tomography (μCT) analysis of excised bones was carried out using the SkyScan1276 CT scanner (Aartselaar, Belgium). Mice bone scanning was performed at 9 μM pixel size, using X-ray source 50 kV, 200 mA. Image slices were reconstructed using the cone-beam reconstruction software version 2.6 based on the Feldkamp algorithm (SkyScan). All analyses were executed on CTAn software, SkyScan. For femur trabecular analysis, 100 slices were selected, leaving 30 slices from the start of the growth plate as a reference point. For cortical analysis, 100 slices were selected. For BMD calculation VOI (volume of interest) was used which was made for trabecular region analysis, using hydroxyapatite phantom rods of 4 mm diameter as standards [39].

Dynamic histomorphometry

For dynamic histomorphometry, undecalcified femora were embedded in acrylic and 50 μm sections were cut by using Isomet-Slow Speed Bone Cutter (Buehler, Lake Bluff, IL) followed by photography using a confocal microscope (LSM 510 Meta, Carl Zeiss, Inc., Thornwood, NY). We enumerated periosteal perimeters, single-labeled surface (sLS), double-labeled surface (dLS) and interlabelled thickness (IrLTh), and these values were employed to calculate mineralizing surface/bone surface (MS/BS), mineral apposition rate (MAR), and bone formation rate (BFR) [40].

Immunohistochemistry

Femur bones were decalcified in decalcifying solution lite (Sigma-Aldrich, St. Louis, MO, USA) for 1 week and embedded in paraffin, 5 μm sections were cut on RM2265 semi-automatic microtome (Wetzlar, Germany). Sections were blocked with a 5% BSA blocking buffer for 1 h at room temperature. After that sections were incubated with the primary antibody of β-catenin (SC7199 Shantacruz 1:100 dilution) overnight. Sections were then incubated with Alexa Fluor 594 (1:200

dilution) for 2 h at room temperature. Sections were washed with PBS and mounted with ProLong Gold Antifade Mountant with DAPI (Life Technologies, USA). Perilipin antibody (NB110-40760SS) was used in 1:50 dilution to detect adipocytes in the bone marrow. Perilipin probed with Alexa Fluor 594 (1:100 dilution) Fluorescence was captured using a fluorescent microscope (Eclipse 80i, Nikon, Tokyo, Japan) with the appropriate filter [39].

Histological analysis of bone

Decalcified femur bones were fixed in 4% paraformaldehyde and then dehydrate in 70% isopropanol. Distal femora were embedded in paraffin wax and 5 µM sections were cut. Sections were de-deparaffinized in xylene and rehydrated in serial changes of isopropanol and water and stained with hematoxylin and eosin, mounted with DPX (Sigma), and was examined under a microscope. Undecalcified femora were embedded in methylmethacrylate and 5 µM sections were cut with Leica RM2265 semi-automatic microtome (Wetzlar, Germany) equipped with a TC-65, a tungsten carbide cutting knife. Sections were undergone deplastication and stained with Vonkossa and Goldner's Trichrome stain. Bone volume (BV/TV) was measured using Bioquant Osteo Software (Bioquant Image Analysis, Nashville, TN, USA) [38, 41].

Serum markers of bone formation and resorption

Bone formation marker osteocalcin (OCN), resorption markers Carboxy-terminal collagen crosslinks (CTX-I), and sclerostin (SOST) were determined by enzyme-linked immunosorbent assay (ELISA) kits according to the manufacturer's protocols from serum. Osteocalcin is exclusively secreted from osteoblasts. A small portion of newly synthesized osteocalcin is released in circulation and can be measured by immunoassays and is a valid marker for bone formation.CTX-1 is a C-terminal cross-linking telopeptide of type I collagen formed after bone resorption [42].

Statistical analysis

Data are expressed as mean ± SEM. The data obtained from experiments were subjected to one-way ANOVA followed by Newman Keul's multiple comparison test of significance using GraphPad prism 5.

Results

Compound 4e preserved cell viability and reduce ROS production in vitro

Dexamethasone (Dex) induced cell death in osteoblasts as assessed by MTT assay. Compound 4e significantly rescued osteoblast from dexamethasone induced cell death at concentrations of 10 nM and 0.1 µM, however, at 0.5 µM and 1 µM concentrations, increase in cell viability was not significant (Fig. 1a). Further, cell apoptosis was assessed and quantified by Annexin-FITC/PI apoptosis assay and compound 4e at 10 nM restored cell viability as more cells in the lower left quadrant (Fig. 1b and c). To further confirm cell apoptosis we used TUNEL assay. There are increased TUNEL positive (green fluorescence) cells in the dex panel (Fig. 1d Dex panel) and compound 4e decreased cell death induced by dex (Fig. 1d Dex + 4e panel). Dexamethasone also increased the intracellular ROS as visible by a greater amount of green fluorescence (H2DCFDA) in dexamethasone treated osteoblasts which were reduced by treatment of compound 4e as visible by lesser green fluorescence at the concentration of 10 nM and 0.1 µM (Fig. 1e and f). The result was confirmed by fluorescent plate reader analysis of H2DCFDA stained cells. Compound 4e decreased the number of H2DCFDA positive cells at 10 nM and 0.1 µM concentrations (Fig. 1g).

Compound 4e abolished dexamethasone induced impairment of osteoblasts differentiation

Treatment of dexamethasone at a concentration of 1 µM impairs the osteogenic potential of osteoblasts in vitro. Treatment for 48 h reduced ALP activity, a crucial osteogenic marker, with a reduced number of alkaline phosphatase (ALP) positive cells. Treatment with compound 4e increased the number of ALP positive cells at the concentrations of 10 nM, 0.1 µM, 0.5 µM, 1 µM (Fig. 2a–c). P-nitrophenyl phosphate (pNPP) assay was also used to assess the ALP activity. As expected Compound 4e overcame the deleterious effect of dexamethasone and rescued osteoblasts with increased ALP activity at a concentration of 10 nM marginally and at the concentrations of 0.1 µM, 0.5 µM, 1 µM significantly (Fig. 2d). Dexamethasone attenuated the mineralization ability of osteoblasts which were restored by compound 4e at aforementioned concentrations (Fig. 2e and f).

Compound 4e increased the expression of osteogenic markers

To assess the effect at the molecular level, we observed that dexamethasone downregulated the expression of RUNX2, BMP2, and ALP genes. Treatment with compound 4e

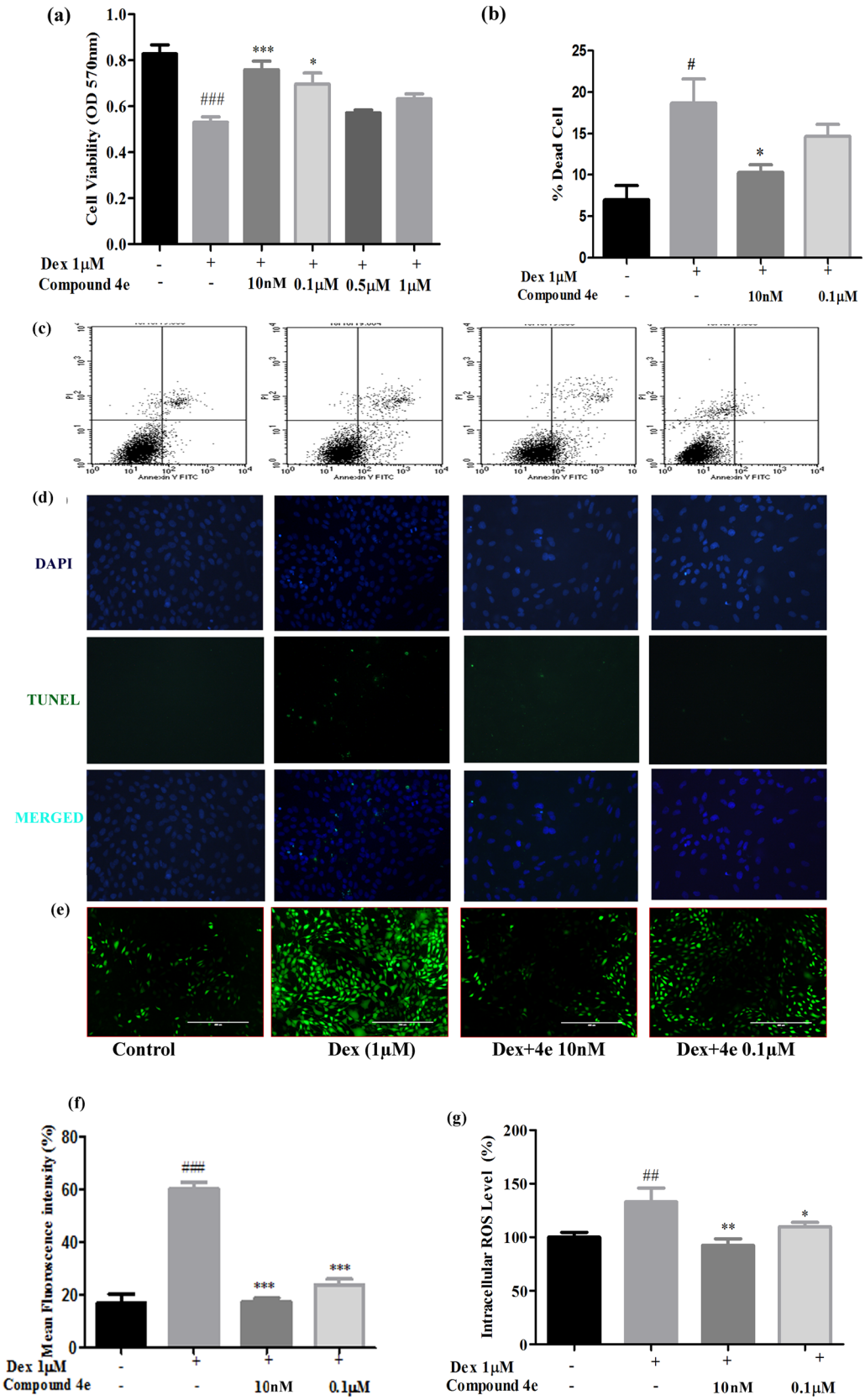
(a)
Cell Viability (OD 570nm)
1.0
0.8
0.6
0.4
0.2
0.0
###
***
*
Dex 1μM - + + + + +
Compound 4e - - 10nM 0.1μM 0.5μM 1μM
(b)
% Dead Cell
25
20
15
10
5
0
#
*
Dex 1μM - + + +
Compound 4e - - 10nM 0.1μM
(c)
PI
Annexin V FITC
(d)
DAPI
TUNEL
MERGED
(e)
Control
Dex (1μM)
Dex+4e 10nM
Dex+4e 0.1μM
(f)
Mean Fluorescence intensity (%)
80
60
40
20
0
###
***
***
Dex 1μM - + + +
Compound 4e - - 10nM 0.1μM
(g)
Intracellular ROS Level (%)
200
150
100
50
0
##
**
*
Dex 1μM - + + +
Compound 4e - - 10nM 0.1μM

◂**Fig. 1** Effect of compound 4e on dexamethasone induced ROS and apoptosis **a** Cell viability assessed by MTT. Compound 4e rescues osteoblast at 10 nM, 0.1 µM. **b** Total dead cell % assessed by **c** Annexin/Pi apoptosis assay. **d** TUNEL assay to detect apoptosis in cells. In dexamethasone treated cells there is higher green (alexa fluor 488) positive cells. Compound 4e decreased apoptosis at 10 nM and 0.1 µM. **e** and **f** Dexamethasone increased intracellular ROS reflected by higher green fluorescence assessed by fluorescent microscope which was attenuated by treatment of compound 4e at 10 nM, 0.1 µM. **g** ROS were also measured separately by spectrophotometer and we had the same result as above. Results were obtained from three independent experiments performed in triplicate and are expressed as Mean ± SEM. $^{\#}p < 0.05$, $^{\#\#}p < 0.01$ $^{\#\#\#}p < 0.001$ versus control, * $p < 0.05$, ** $p < 0.01$ *** $p < 0.001$ versus dexamethasone

reversed the effect of dexamethasone and increased the mRNA expression of RUNX2 by 2.4, 1.6, 1.7, and 2.11 folds at the concentrations of 10 nM, 0.1 µM, 0.5 µM, 1 µM respectively (Fig. 3a). A similar increase was observed for BMP2 by approximately 2.3, 1.5, 3.1, and 2.9 folds (Fig. 3b) and for ALP by 1.6, 2.1, at 10 nM and 0.1 µM. (Fig. 3c). Compound 4e also maintained the RANKL/OPG balance by downregulating RANKL and increasing the mRNA expression of OPG at the concentrations of 10 nM, 0.1 µM, 0.5 µM, 1 µM significantly (Fig. 3d and e).

The functions of these proteins were also altered by dexamethasone as evidenced in western blots (Fig. 4a). Dexamethasone showed its negative effect by downregulating RUNX2 (Fig. 4a and d) via inhibiting BMP2 (Fig. 4a and b) signaling. Compound 4e restored the BMP2/SMAD1/5/8 (Fig. 4a and c) signaling pathway and increased RUNX2 expression at 10 nM and 0.1 µM concentrations (Fig. 4d). Further, we confirmed this result by immunocytochemistry, dexamethasone downregulated RUNX2 expression in the nuclei of the osteoblast cells as visible by less green fluorescence in dexamethasone treated cells, and treatment of compound 4e restored the expression of RUNX2 (Fig. 4e).

Compound 4e utilized the Wnt/β-catenin pathway to extenuate the dexamethasone effect in vitro

We assessed the possible mechanism by which compound 4e could ameliorate dexamethasone induced inhibition of osteoblast function to strengthen our claim. Wnt/β-catenin is a major pathway by which dexamethasone exerts its effects. Real-time PCR data shows that dexamethasone increased expression of Wnt inhibitor SOST and downregulated expression of β-catenin. Compound 4e decreased the expression of SOST by 9.3, 6, 3.7, and 4.3 fold at the concentrations of 10 nM, 0.1 µM, 0.5 µM, 1 µM respectively in comparison to dexamethasone treated group (Fig. 5a). Compound 4e increased an essential mediator of Wnt signaling β-catenin by approximately 2.5, 2.1, 2.2 fold at the concentrations of 10 nM, 0.1 µM, 0.5 µM, respectively (Fig. 5b). Immunoblotting confirmed the results as dexamethasone increased the expression of SOST (Fig. 5c and d), and attenuating phosphorylation of GSK3-β (Ser9) (Fig. 5c and e). Activation of GSK3-β phosphorylated β-catenin and its degradation. Treatment with compound 4e activated the Ser9 phosphorylation of GSK3-β thus its inactivation and increased the expression of β-catenin (Fig. 5c and f). Compound 4e also increased the β-catenin nuclear localization which is an important step for canonical Wnt signaling. We stained β-catenin with Alexa fluor 594 and observed its co-localization with DAPI (Blue) which gives purple color. Dexamethasone inhibits the nuclear localization and compound 4e enhanced this at 10 nM and 0.1 µM (Fig. 5g).

Effect of compound 4e on trabecular bone microarchitecture

To assess the effect of compound 4e at the bone microarchitectural level we analyzed the distal femoral metaphysis by microCT after treatment with methylprednisolone (MP), a synthetic glucocorticoid that was used for in vivo administration. Compound 4e protected bone microarchitecture from glucocorticoid induced bone loss as shown in 3D microCT images (Fig. 6a). Methylprednisolone decreased BMD (Bone mineral density) by approximately 23% (Fig. 6b), bone volume (BV/TV) by 39.5% (Fig. 6c), trabecular thickness (Tb.Th) by 22.9% (Fig. 6d), trabecular number (Tb.N) by 22.8% (Fig. 6e) and increased trabecular separation (Tb. Sp) (Fig. 6f) and SMI (Fig. 6g) by 32.6%, 72% respectively in comparison to control animals. Oral dosing of compound 4e at 2.5 mg kg^{-1} and 5 mg kg^{-1} concentrations restored the bone microarchitecture by increasing BMD by approximately 31.7% and 43.4%, BV/TV by 62% and 74.6%, Tb.Th by 9.5% and 21.4%, Tb. N by 39.9% and 48.4% and by decreasing Tb.Sp by 28.2% and 29.8%, SMI by 59.8% and 64% respectively in comparison to MP group.

Effect of compound 4e on cortical bone and dynamic histomorphometry

3D representative images of Cortical bone at mid femoral diaphysis showed that compound 4e abrogated bone loss effect of methylprednisolone (Fig. 7a). Methylprednisolone reduced the cortical thickness of bone by 14% and increase cortical porosity by 17% thus making the bones fragile. Oral dosing of compound 4e rescued the bones by increasing the cortical thickness at both concentrations of 2.5 and 5 mg kg^{-1} by 20% and 21% respectively and decreased cortical porosity by 10.8% at 5 mg kg^{-1} dose (Fig. 7b and c). Through dynamic histomorphometry studies, we showed the effect of methylprednisolone in reducing bone formation in animals as assessed by a single and discontinuous calcein green fluorescent line (Fig. 7d). Administration of Compound 4e attenuated the inhibited bone formation at

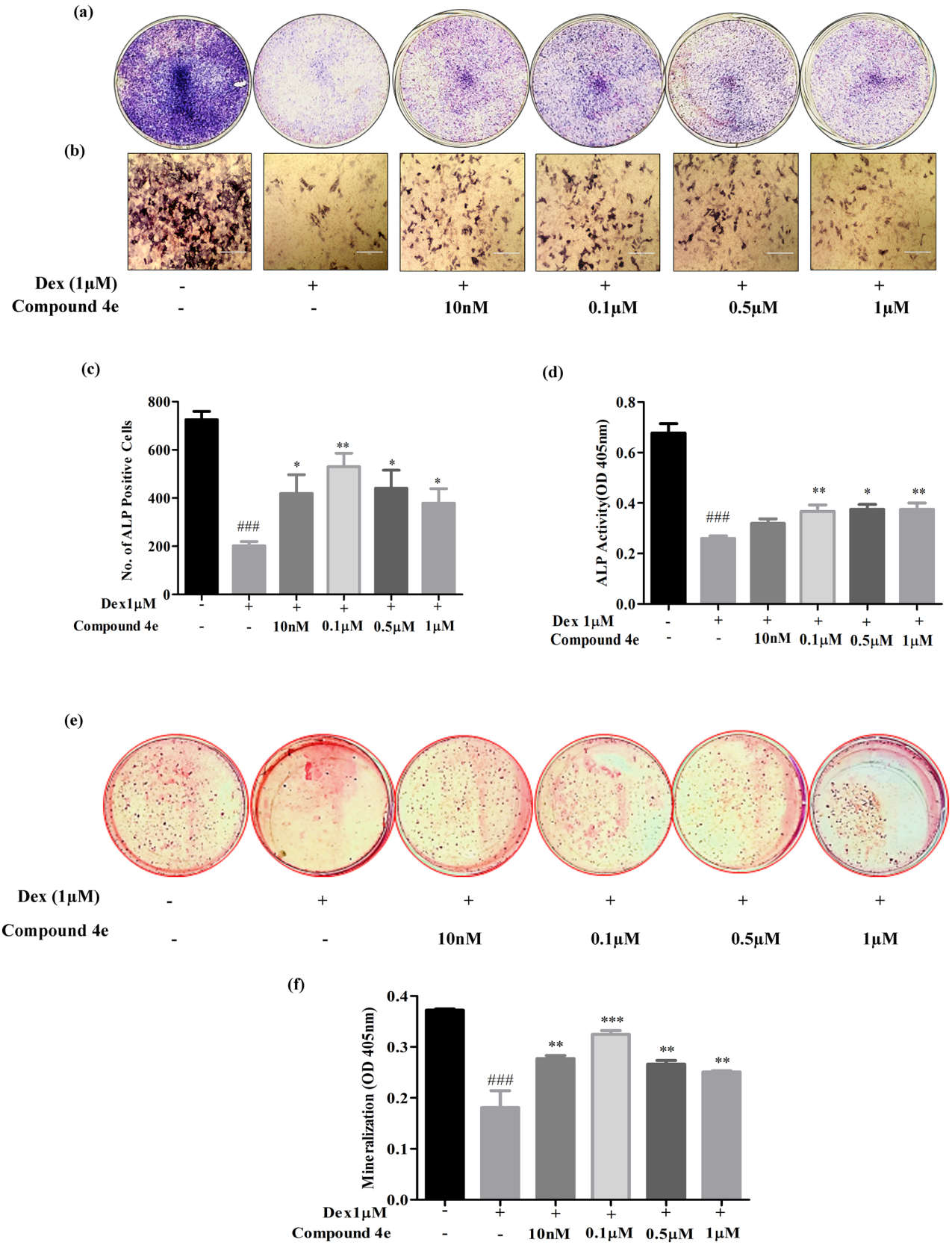
(a)
(b)
Dex (1μM) - + + + + +
Compound 4e - - 10nM 0.1μM 0.5μM 1μM
(c)
No. of ALP Positive Cells
800
600
400
200
0
###
*
**
*
*
Dex1μM - + + + + +
Compound 4e - - 10nM 0.1μM 0.5μM 1μM
(d)
ALP Activity(OD 405nm)
0.8
0.6
0.4
0.2
0.0
###
**
*
**
Dex 1μM - + + + + +
Compound 4e - - 10nM 0.1μM 0.5μM 1μM
(e)
Dex (1μM) - + + + + +
Compound 4e - - 10nM 0.1μM 0.5μM 1μM
(f)
Mineralization (OD 405nm)
0.4
0.3
0.2
0.1
0.0
###
**
***
**
**
Dex1μM - + + + + +
Compound 4e - - 10nM 0.1μM 0.5μM 1μM

◂**Fig. 2** Compound 4e increased ALP and mineralization. **a** Representative ALP staining (NBT/BCIP) macroscopic images and **b** at × 10 magnification. **c** Quantification of ALP staining by Image Pro software. **d** ALP activity also confirmed separately by pNPP method. Dexamethasone decreased ALP activity and treatment of compound 4e at 10 nM, 0.1 µM, 0.5 µM and 1 µM concentrations increase osteoblast differentiation. **e** Dexamethasone diminished mineralization capacity of osteoblasts which were restored by compound 4e at 10 nM, 0.1 µM, 0.5 µM and 1 µM concentrations. **f** Quantification of mineralization nodules. Results were obtained from three independent experiments performed in triplicate and are expressed as Mean ± SEM. $^{\#}p < 0.05$, $^{\#\#}p < 0.01$ $^{\#\#\#}p < 0.001$ versus control, $^{*}p < 0.05$, $^{**}p < 0.01$ $^{***}p < 0.001$ versus dexamethasone

2.5 mg kg^{-1} and 5 mg kg^{-1} doses (Fig. 7d). Methylprednisolone inhibited mineralizing surface/bone surface (MS/BS) (Fig. 7e) and mineral accrual rate (MAR) (Fig. 7f), and thus bone formation rate (BFR) (Fig. 7g). Compound 4e dosing for 4 weeks increased the MS/BS, MAR, and BFR.

Compound 4e employed Wnt/β-catenin pathway to ameliorate adverse effect of glucocorticoid on bone in vivo

We observed that administration of glucocorticoid increased SOST mRNA expression in bone by 3.0 folds as compared to animals not receiving glucocorticoid. Dosing of animals with 2.5 mg kg^{-1} and 5 mg kg^{-1} compound 4e downregulated SOST by 7.56 folds (Fig. 8a).

When we estimated circulating levels of SOST in the serum by sandwich ELISA we observed increased levels in the MP group by approximately 381%. Compound 4e at 2.5 mg kg^{-1} and 5 mg kg^{-1} dose reduced SOST level by 86% and 81.5% respectively (Fig. 8b). Immunohistochemistry data unfolds that the expression of the β-catenin protein, a central member of Wnt/β-catenin signaling was found to be abundant in the Control group of mice (red fluorescence alexa fluor 594) co-localized with DAPI (Blue) thus got purple color in merged panel. Expression of β-catenin was decreased in the MP group. The decreased expression was significantly reversed in the co-treatment groups of MP and compound at the doses 2.5 mg kg^{-1} and 5 mg kg^{-1} body weight (Fig. 8c). Thus, making our findings robust and consistent with the previous data exhibiting the osteogenic potential of our compound following the Wnt/β-catenin signaling pathway.

Compound 4e abrogated methylprednisolone induced bone marrow adiposity

Continuous exposure to Methylprednisolone increased bone marrow adipocytes. We stained bone tissue with hematoxylin and eosin and found the globular spaces in the bone marrow of MP treated animals (Fig. 9a). These globular spaces (adipocyte ghosts) depict adipocytes in the bone marrow. We performed IHC to show bone marrow adiposity with perilipin antibody, tagged with Alexa fluor 594, which is a surface marker of lipid droplets. In MP treated animals there is an enhanced number of adipocytes thus lipid droplets. Compound 4e abrogated this effect at 2.5 and 5 mg kg^{-1} doses (Fig. 9b).

Compound 4e increased bone formation and inhibit osteocyte death

It is well established that glucocorticoid alters osteocyte function by inducing apoptosis. H&E staining also demonstrated increased empty lacunae in the trabecular bone of the MP group suggesting osteocyte death. Treatment of the compound at the above-mentioned doses 2.5 mg kg^{-1} and 5 mg kg^{-1} reduced the increased number and size of empty lacunae, representative of osteolysis (Fig. 10a). We also employed TUNEL to show apoptosis of osteocytes in bone tissue. There are increased TUNEL positive cells in the MP group in comparison to the control. Compound 4e decreased osteocyte apoptosis reflected by lesser TUNEL positive cells in comparison to the MP group (Fig. 10b).

Effect of compound 4e on bone histology and serum markers

Von-Kossa and Goldner's trichrome (GT) staining of the femur sections revealed the inadequate number and discontinuous orientation of the trabeculae in the MP treated mice when compared to the Control (without MP) (Fig. 11a and b MP panel). Treatment of the compound at doses 2.5 mg kg^{-1} and 5 mg kg^{-1} body weight reversed the deleterious impact caused by MP on the mineralized matrix. Reversal of the disrupted trabecular bone is seen in terms of increased trabecular thickness and number as observed visually in the histological sections (Fig. 11a and b). We quantified BV/TV in GT stained sections by BIOQUANT OSTEO software (Fig. 11c).

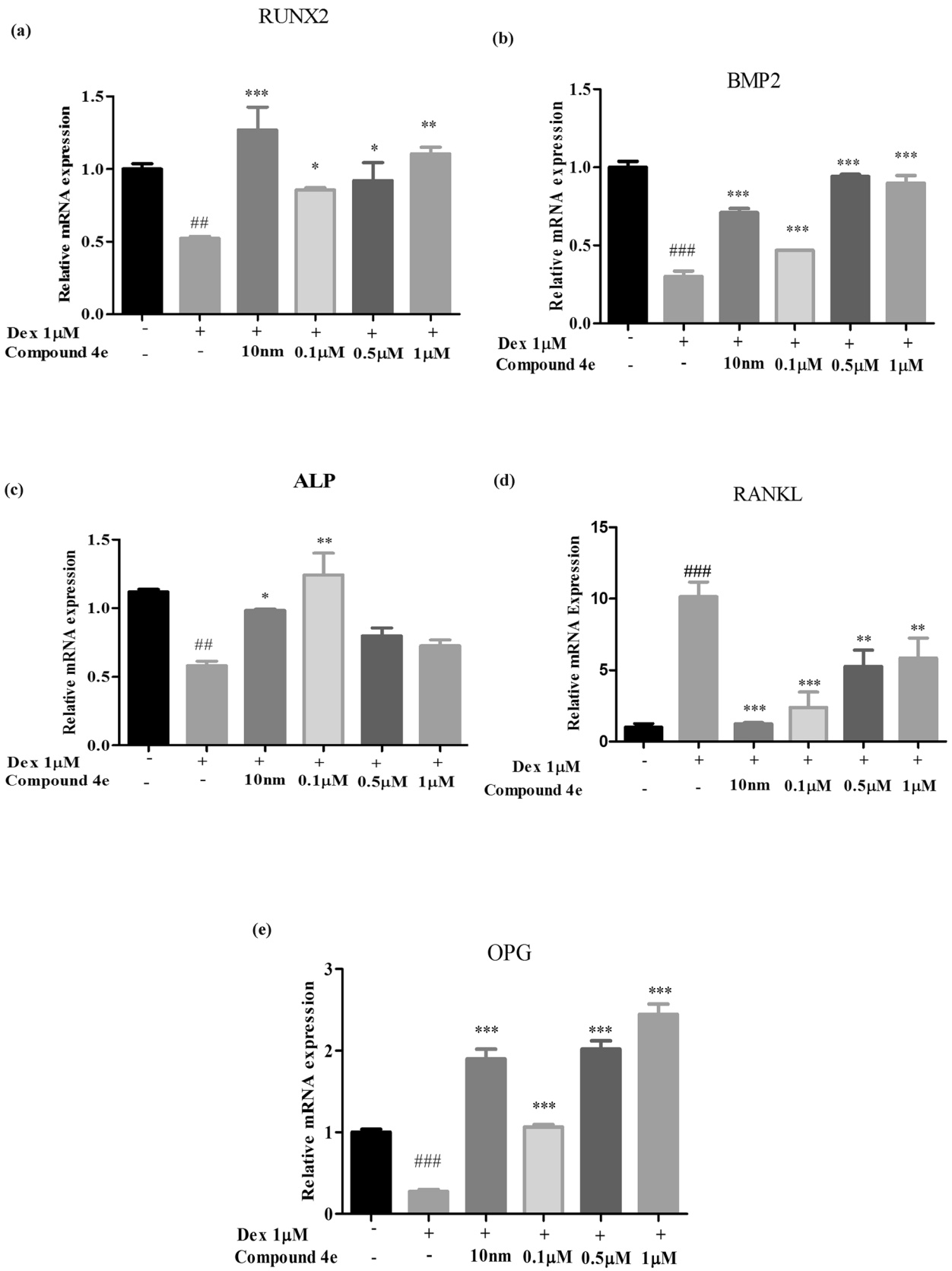
(a)
RUNX2
Relative mRNA expression
1.5
1.0
0.5
0.0
##
***
*
*
**
Dex 1μM - + + + + +
Compound 4e - - 10nm 0.1μM 0.5μM 1μM
(b)
BMP2
Relative mRNA expression
1.5
1.0
0.5
0.0
###
***
***
***
***
Dex 1μM - + + + + +
Compound 4e - - 10nm 0.1μM 0.5μM 1μM
(c)
ALP
Relative mRNA expression
1.5
1.0
0.5
0.0
##
*
**
Dex 1μM - + + + + +
Compound 4e - - 10nm 0.1μM 0.5μM 1μM
(d)
RANKL
Relative mRNA Expression
15
10
5
0
###
***
***
**
**
Dex 1μM - + + + + +
Compound 4e - - 10nm 0.1μM 0.5μM 1μM
(e)
OPG
Relative mRNA expression
3
2
1
0
###
***
***
***
***
Dex 1μM - + + + + +
Compound 4e - - 10nm 0.1μM 0.5μM 1μM

◂**Fig. 3** Compound 4e ameliorated dexamethasone induced inhibition of osteogenic genes. **a** Compound 4e increased mRNA expression of RUNX2 **b** BMP2, **c** ALP which were down-regulated by dexamethasone. **d** Compound 4e maintained RANKL/OPG ratio by downregulating RANKL and **e** increasing OPG expression at 10 nM, 0.1 μM, 0.5 μM and 1 μM concentrations. Results were obtained from three independent experiments performed in triplicate and are expressed as Mean ± SEM. $^{\#}p < 0.05$, $^{\#\#}p < 0.01$ $^{\#\#\#}p < 0.001$ versus control, $^{*}p < 0.05$, $^{**}p < 0.01$ $^{***}p < 0.001$ versus dexamethasone

Bone turnover markers in serum were measured in the control (untreated) and treatment groups after 28 days of glucocorticoid administration. Serum CTX-I was robustly increased in the MP group mice than control. The percentage increase in the level of CTX-I is approximately 45% in the MP group in comparison to control. In treatment groups of 2.5 mg kg^{-1} and 5 mg kg^{-1} with compound 4e a significant reduction to 23.2% and 29.8% was observed Fig. 11d). A well-established key osteogenic marker OCN was also evaluated and results indicated a decrease in OCN level in the MP group by 51.9% whereas our treatment group of 2.5 mg kg^{-1} and 5 mg kg^{-1} significantly increased the downregulated level by 58.6% and 71.2% respectively (Fig. 11e). This data indicated an osteoanabolic effect of compound 4e.

Discussion

Bone loss due to long term use of glucocorticoids (GC) occurs by inhibiting osteoblast survival and function. Excess glucocorticoid acts directly on osteoblast and osteocytes and promotes their death. Studies on transgenic mice show that overexpressing 11β-hydroxysteroid dehydrogenase type-2 converts active glucocorticoid into inactive form preventing osteoblast death [43]. Dexamethasone induces osteoblast apoptosis via GSK3β and Caspases activation [44]. Through this study, we have shown the preventive effect of compound 4e on GC induced bone loss in mice. GIOP is marked by loss of bone mineral density (BMD) and deterioration of cancellous and cortical microstructure [42, 45, 46]. These overall changes in bone volume are due to loss in trabecular thickness (Tb. Th) and trabecular number (Tb. N). Furthermore, erosion of the trabeculae results in increased trabecular separation (Tb. Sp). A higher ratio of rod-shaped trabeculae in comparison to plates in glucocorticoid treated mice indicated poor geometric disposition because rods are mechanically inferior to plates predisposing one to lower bone strength. We observed that compound 4e restored the trabecular microstructure by increasing the trabecular thickness and number and also restored plate like trabaculae. Glucocorticoids initially affect trabecular bone but with long exposure, cortical bone is also affected with reduced bone load bearing capacity. There is evidence that glucocorticoids decreased cortical thickness and increase the porosity of cortical bone [47, 48]. Treatment with compound 4e ameliorated the effect of GC and maintained cortical thickness and cortical porosity. Decreased cortical thickness is a reflection of the lower bone formation rate. There was lower mineralizing surface hence mineral apposition rate in GC treated group due to lower osteoblast activity and higher osteoclast activity as observed by single or discontinuous calcein labeling as compared to control animals. Our data suggest that compound 4e increased mineralizing surface and mineral apposition rate at doses of 2.5 mg kg^{-1} and 5 mg kg^{-1} ultimately increasing the bone formation rate.

Wnt signaling is vital for osteoblastogenesis and glucocorticoids use this pathway to stimulate mesenchymal stem cells in favor of osteoblasts at the physiological level and the same pathway is inhibited when glucocorticoid is in excess [13, 14]. Removal of Wntless (Wls), a chaperon required for normal secretion of Wnt ligand from cells, resulted in severe osteoporosis due to less bone formation and high bone resorption [49]. In vitro and in vivo studies have established that glucocorticoid administration suppresses Wnt signaling [16, 50]. In agreement with previous studies, we also observed suppressed Wnt signaling pathways. The inhibitory effect of glucocorticoid on the Wnt pathway is mediated through increased expression of SOST [51]. Compound 4e attenuated the inhibitory effect of glucocorticoid on the Wnt pathway by inhibiting SOST mRNA and protein expression. We also found increased serum levels of SOST in glucocorticoid treated mice which were reduced by compound 4e. BMP2 protein is an important regulator of osteoblast function and bone formation [52–54]. Several studies have reported that glucocorticoid negatively affects BMP2/SMAD pathway and restored osteogenic property after treatment of recombinant BMP2 protein [55–57]. In our study treatment of dexamethasone decreased BMP2/SMAD1/5 pathway. Treatment with compound 4e restored the BMP2 signaling pathway by increasing its expression at mRNA and protein levels.

The above observations were confirmed with the circulating clinical biomarkers, the bone resorption marker CTX-I and bone formation marker Osteocalcin level in serum was perturbed in GIOP [42, 58]. Oral dosing of our compound promoted bone formation by decreasing CTX-I level and increasing OCN level in serum.

Compound 4e belongs to the benzofuran pyran chemical group. Benzofuran is a member of heterocyclic compounds. Heterocyclic compounds provide scaffolds on which pharmacophores can arrange to yield potent and selective drugs [59]. With precise reference to the pharmaceutical industry, Heterocyclic motifs are particularly prevalent in the industry, with over 60 percent of top retail drugs having at least one heterocyclic nucleus as part of the complete topography of the compound [60]. Compounds containing heterocyclic moieties also exhibit improved solubility and can promote salt formation properties, both of which are known to be essential for

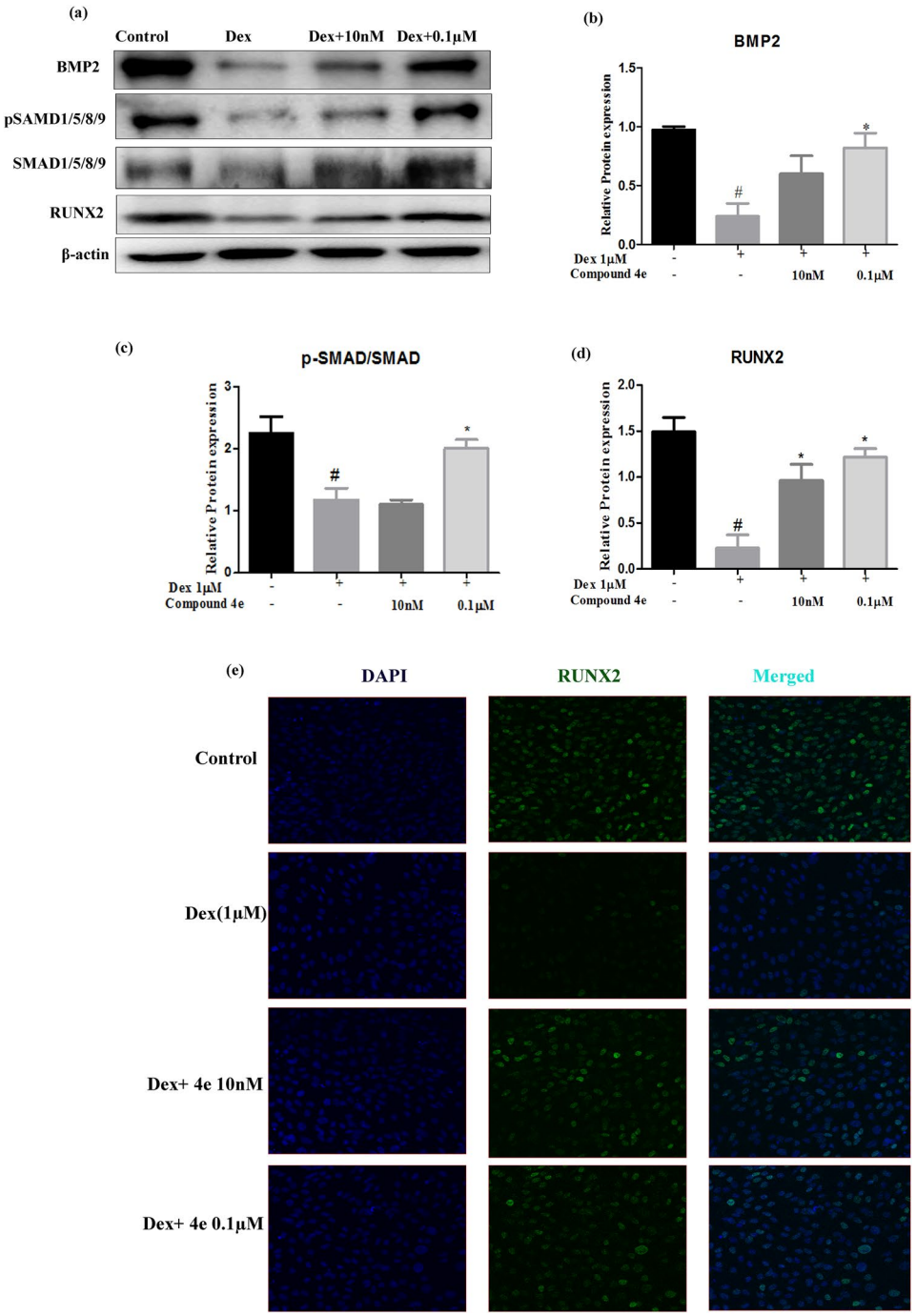

Fig. 4 Compound 4e maintained RUNX2 and BMP2 at protein level. **a** and **b** Compound 4e increased BMP2 protein expression and phosphorylation of **a** and **c** SMAD 1/5/8 at 0.1 μM thus increasing, **a** and **d** RUNX2 at 10 nM, and 0.1 μM concentration. **e** Dexamethasone downregulated RUNX2 expression marked by lower green fluorescence and treatment of compound 4e increased RUNX2 expression reflected by higher green fluorescence at 10 nM, 0.1 μM concentration. Results were obtained from three independent experiments performed in triplicate and are expressed as Mean ± SEM. $^{\#}p < 0.05$ versus control, $^{*}p < 0.05$ versus dexamethasone

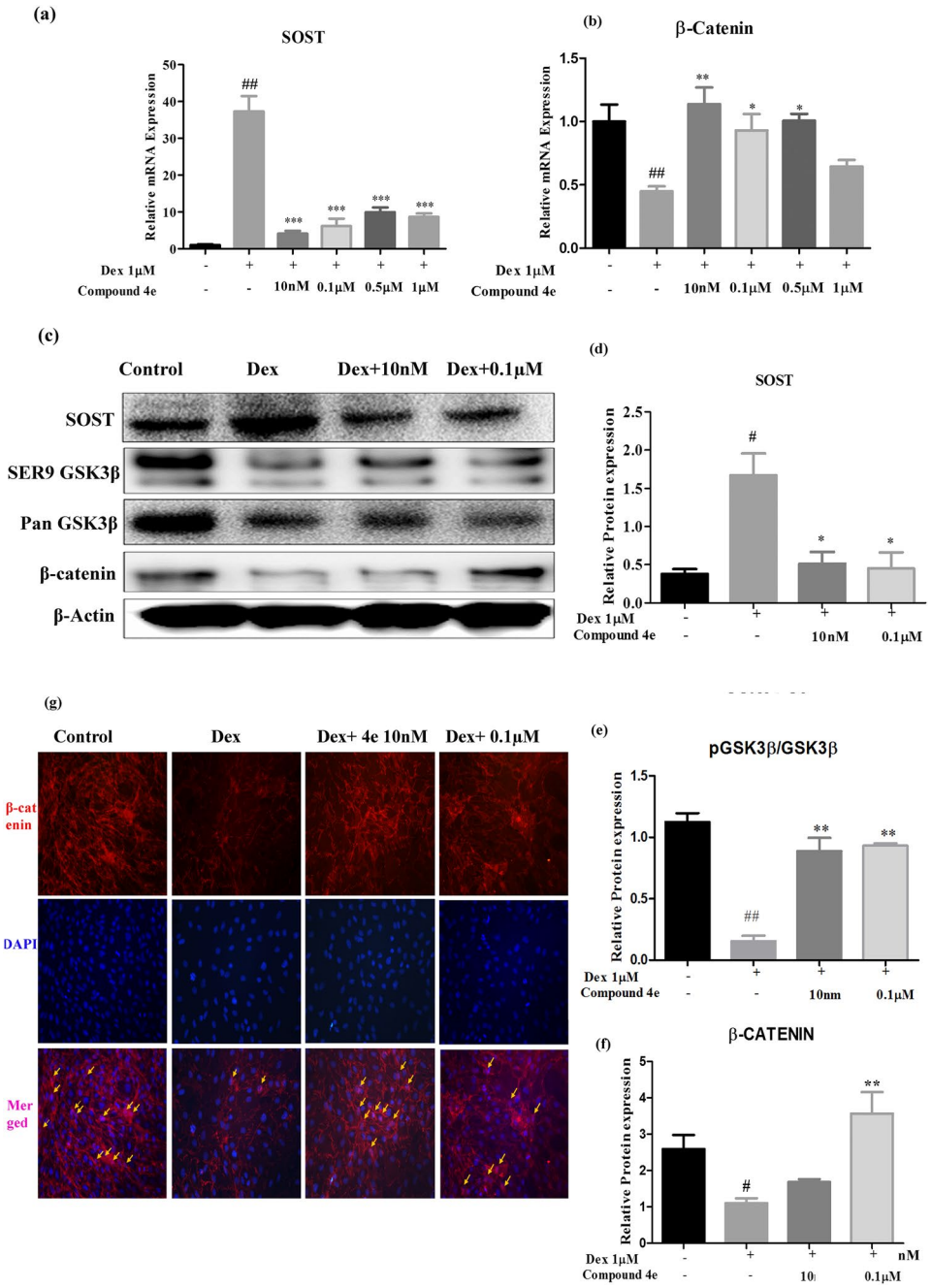

Fig. 5 Compound 4e employed the Wnt/β-catenin pathway to attenuate dexamethasone effect in osteoblasts. **a** Dexamethasone increased the expression of Wnt inhibitor SOST. Compound 4e downregulated SOST expression at 10 nM, 0.1 μM, 0.5 μM and 1 μM concentrations. **b** Compound 4e increased β-catenin expression at 10 nM, 0.1 μM, 0.5 μM, and 1 μM concentrations which were reduced by dexamethasone. **c** and **d** Compound 4e downregulated SOST protein expression and increased inhibition of **c** and **e** GSK3-β thus increasing nuclear localization of (c and f) β-catenin. There is a lesser purple signal (alexa fluor 594 + DAPI) (**g**) in the dex treated group. Compound 4e increased nuclear localization as greater red signal localizes with DAPI. Results were obtained from three independent experiments performed in triplicate and are expressed as Mean ± SEM. $^{\#}p < 0.05$, $^{\#\#}p < 0.01$ $^{\#\#\#}p < 0.001$ versus control, $^{*}p < 0.05$, $^{**}p < 0.01$ $^{***}p < 0.001$ versus dexamethasone

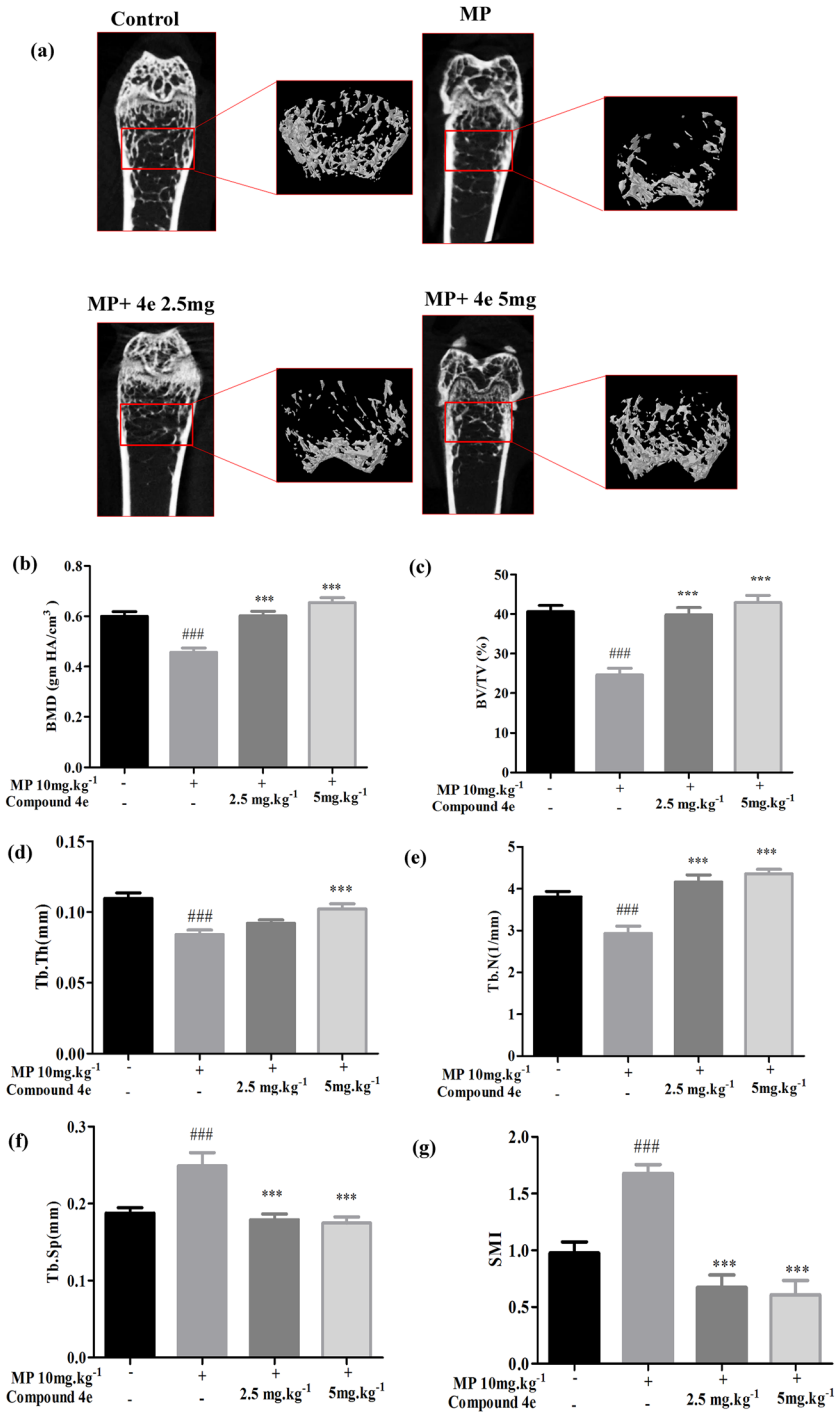

Fig. 6 Compound 4e improved micro architecture of femur in MP administered groups. Images obtained from Micro-CT. **a** Represented 3D/2D Images of femur trabecular of all groups. Femur trabecular parameters were measured. **b** Volumetric BMD (g HA/cm^3), **c** BV/TV %, **d** Tb.Th (mm), **e** Tb.N (1/mm), **f** Tb.Sp (mm), and **g** SMI of animals of study groups were measured. Compound 4e was able to restore microarchitectural parameters in MP treated animals. All values are expressed as Mean ± SEM (n = 8/group); $^{\#}p < 0.05$, $^{\#\#}p < 0.01$, $^{\#\#\#}p < 0.001$ compared control group to the MP group.*$p < 0.05$, **$p < 0.01$, ***$p < 0.001$ compared MP to the 4e treated groups

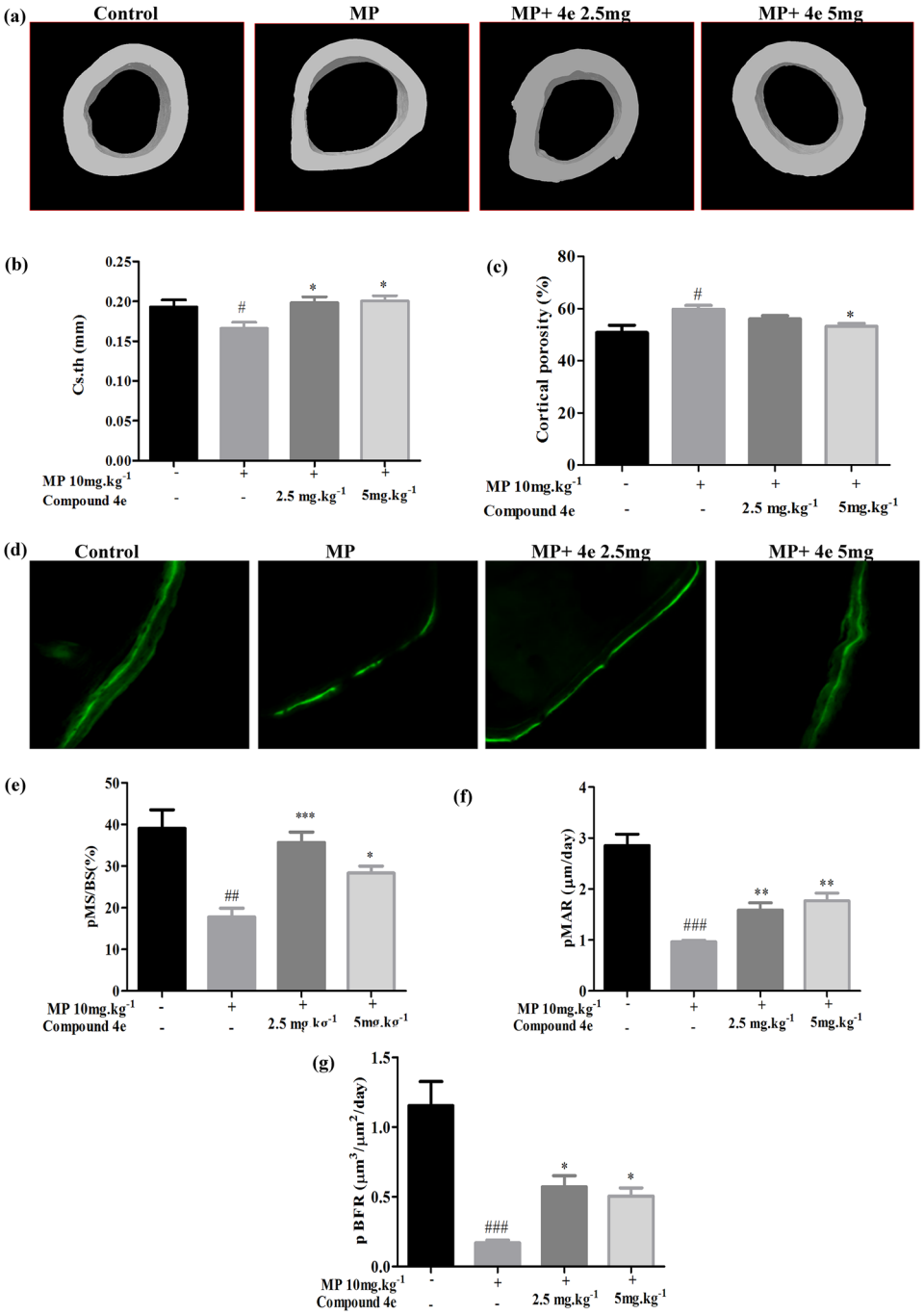

Fig. 7 Compound 4e rescue cortical bone from thinning and increased bone formation rate. **a** Representative 3D images of cortical bone. Oral dosing of compound 4e at 2.5 mg.kg^{-1} and 5 mg kg^{-1} doses increased **b** cortical thickness and **c** decreased cortical porosity. **d** Representative images of calcein double labelling. Dexamethasone inhibits bone formation marked by single and discontinuous label. Compound 4e restored the bone formation at 2.5 mg kg^{-1} and 5 mg kg^{-1}. Compound 4e increased **e** MS and **f** MAR thus increased **g** BFR at 2.5 mg kg^{-1} and 5 mg kg^{-1}. All values are expressed as Mean ± SEM (n = 8/group); $^{\#}P < 0.05$, $^{\#\#}P < 0.01$, $^{\#\#\#}P < 0.001$ compared control group to the MP group.*P < 0.05, **P < 0.01, ***P < 0.001 compared MP to the 4e treated groups

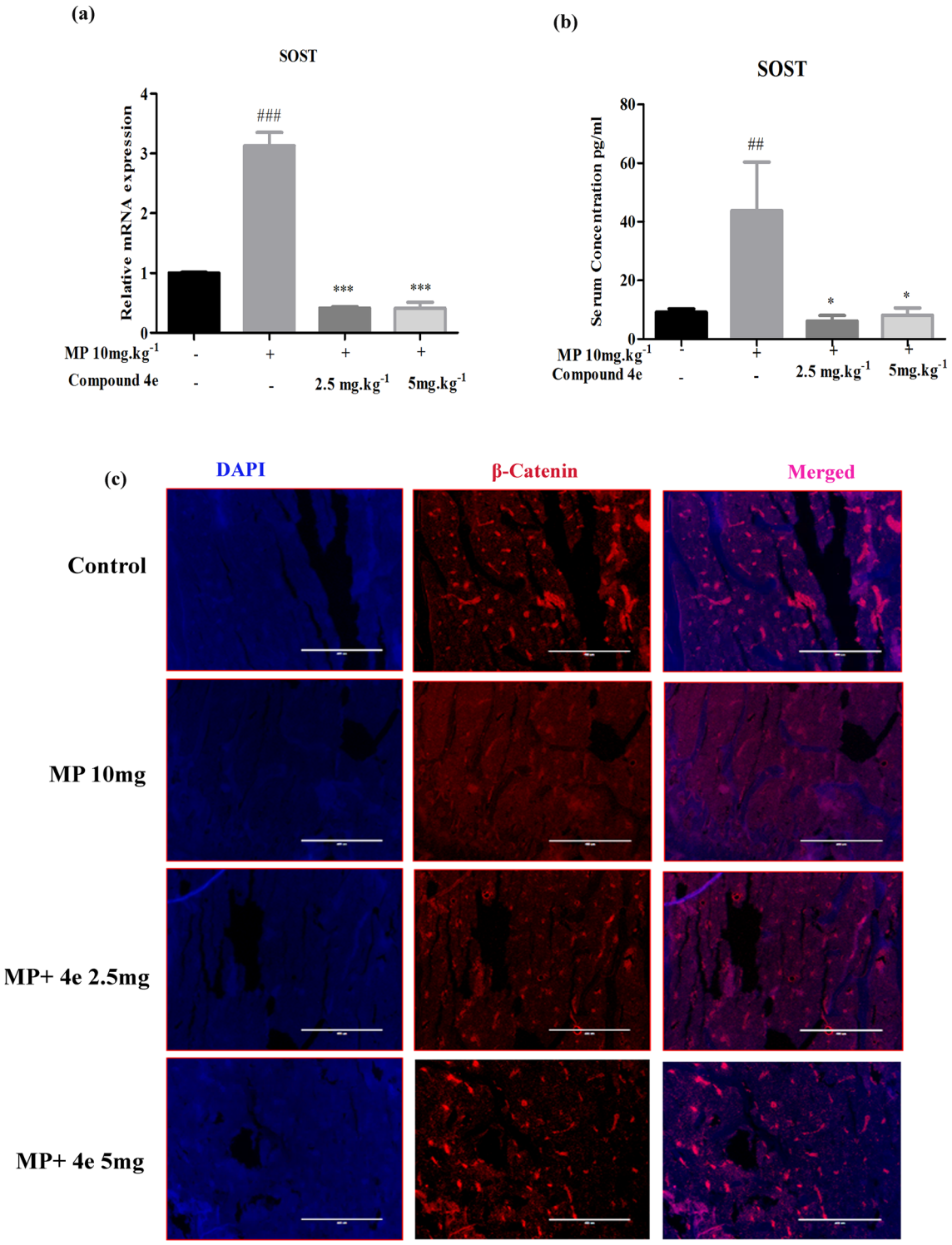

Fig. 8 Compound 4e maintained Wnt/β-catenin pathway by reducing SOST in mice. **a** Glucocorticoid increased SOST mRNA and **b** serum level which were reduced by compound 4e at 2.5 mg kg^{-1} and 5 mg kg^{-1}. **c** Immunohistochemistry showed markedly reduced β-catenin in MP treated mice reflected by lesser red fluorescence which were abrogated by compound 4e dosing. All values are expressed as Mean ± SEM (n = 3/group); $^{\#}P < 0.05$, $^{\#\#}P < 0.01$, $^{\#\#\#}P < 0.001$ compared control group to the MP group.*P < 0.05, **P < 0.01, ***P < 0.001 compared MP to the 4e treated groups

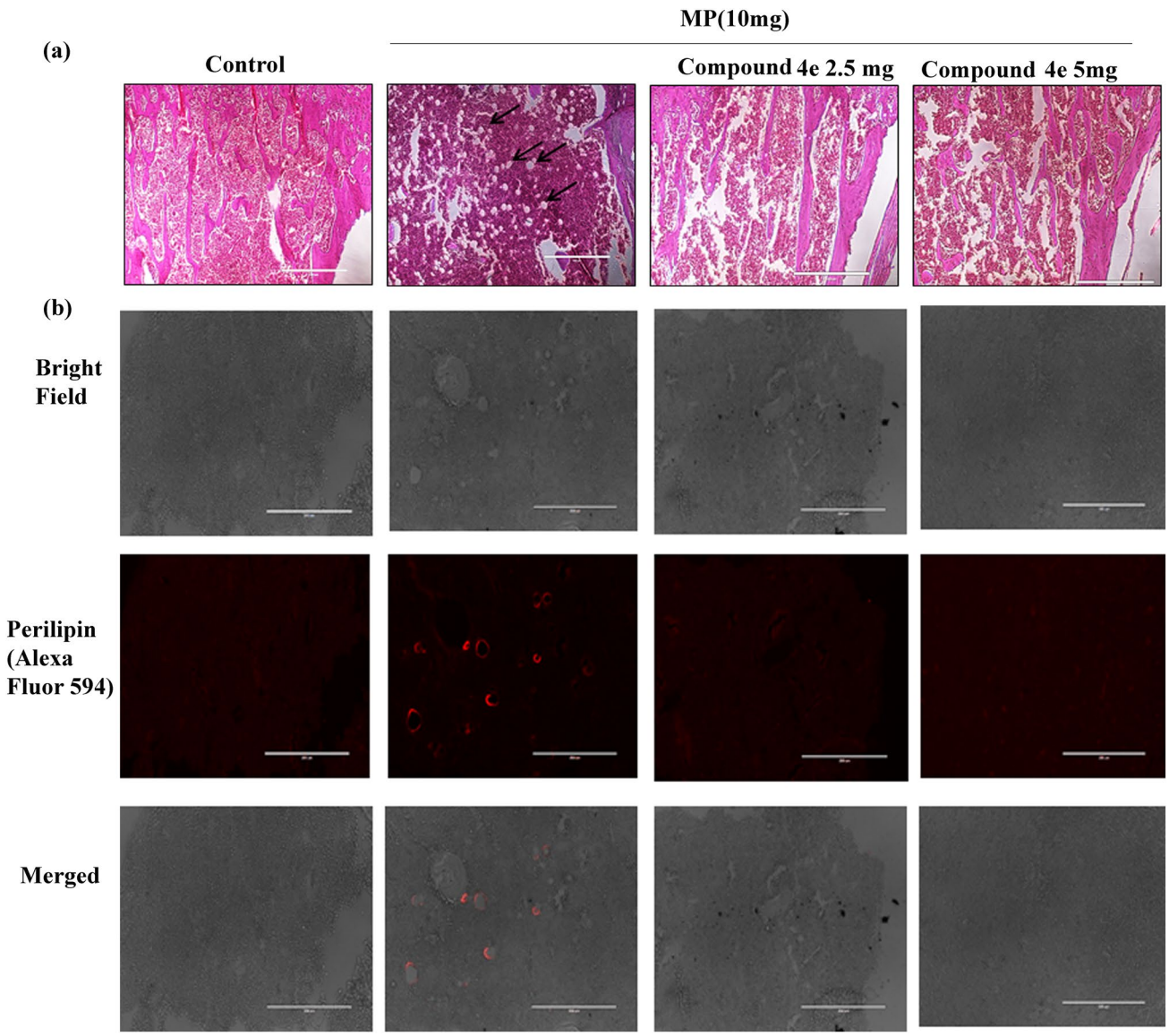

Fig. 9 Compound 4e diminishes bone marrow adiposity. **a** Higher globular spaces visualized with H&E staining (**b**) and perilipin positive cells (Alexa fluor 594) reflecting higher adipocytes in MP bone marrow. Compound 4e diminishes bone marrow adiposity at 2.5 mg kg^{-1} and 5 mg kg^{-1}

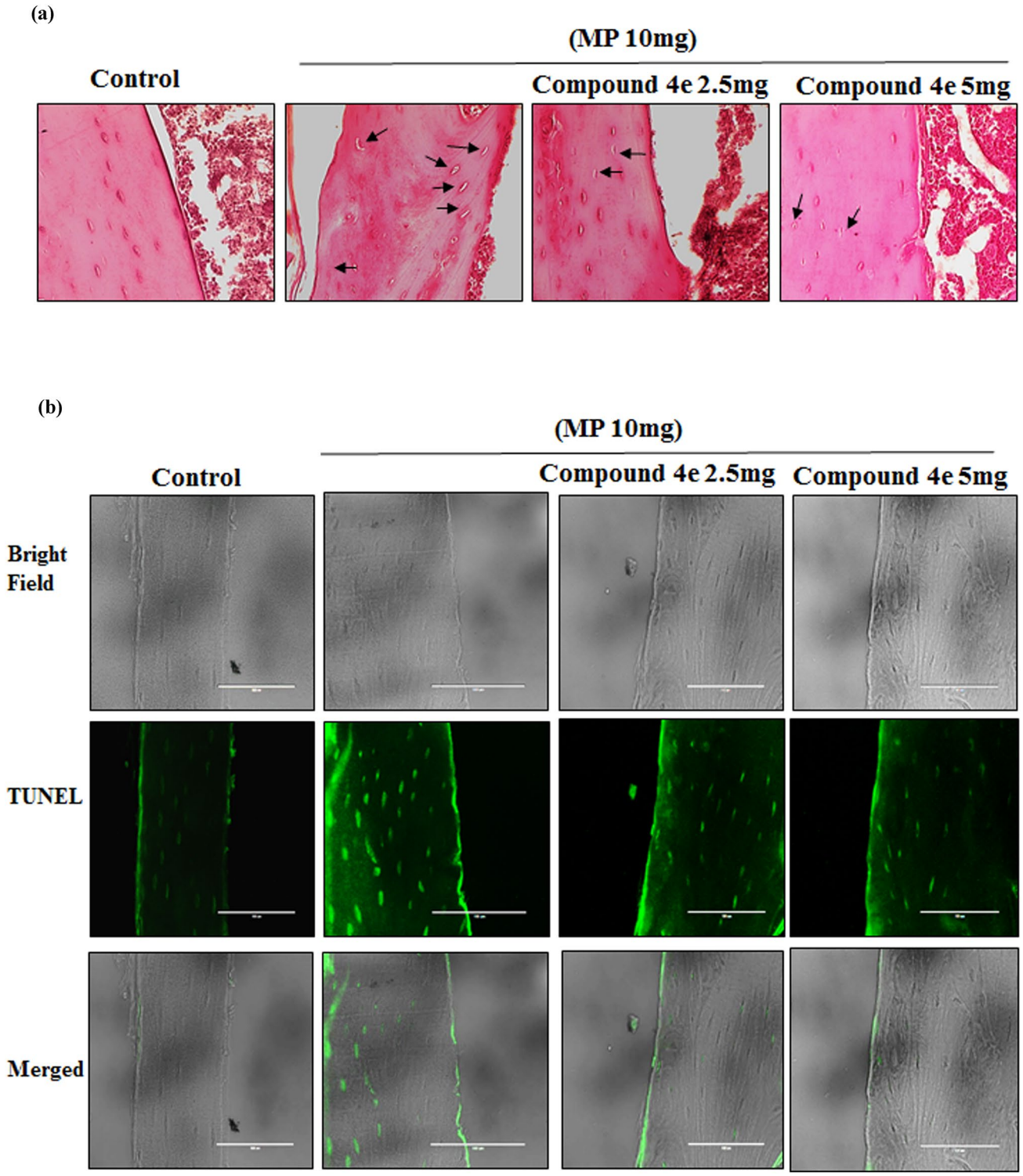

Fig. 10 Compound 4e decreased osteocyte apoptosis in bone tissue. **a** Greater empty lacunae visualized with H&E staining (**b**) and TUNEL positive cells (Alexa fluor 488) reflecting higher osteocyte apoptosis in MP bone tissue. Compound 4e diminishes osteocyte apoptosis at 2.5 mg kg^{-1} and 5 mg kg^{-1}

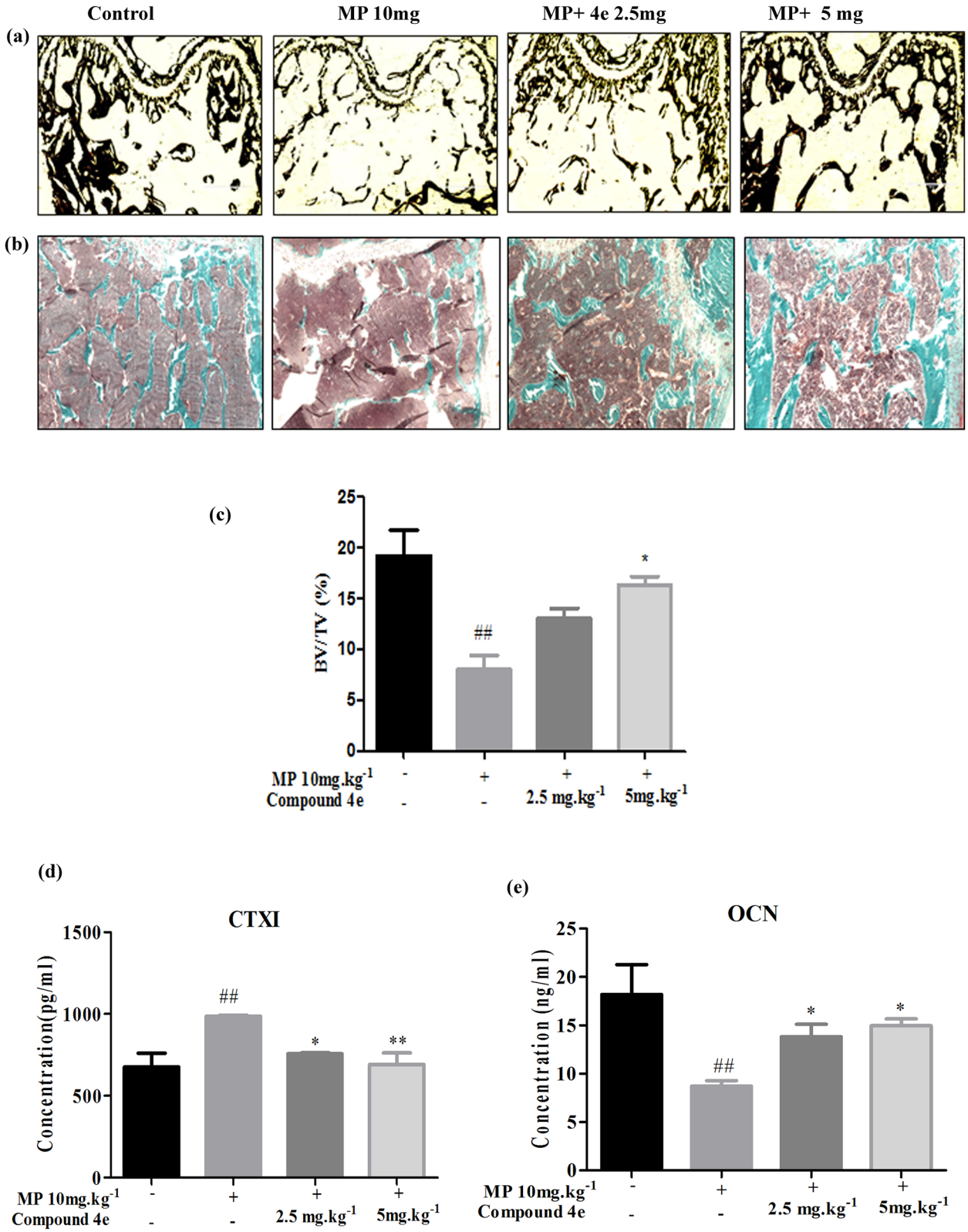

Fig. 11 Compound 4e improved histological architecture of trabecular and serum markers in MP administered groups. **a** Von kossa staining (× 10). **b** GT stain shows trabecular loss in MP group which were recovered in 4e treated groups. **c** Trabecular bone were quantified as BV/TV (%) by Bioquant osteo software. In serum of MP only group, collagen degradation marker, **d** CTX-I increased while bone formation marker, **e** OCN was decreased. Both markers are restored in 4e treated groups. All values are expressed as Mean ± SEM (n = 3/group); $^{\#}P < 0.05$, $^{\#\#}P < 0.01$, $^{\#\#\#}P < 0.001$ compared control group to the MP group.*$P < 0.05$, **$P < 0.01$, ***$P < 0.001$ compared MP to the 4e treated groups

oral absorption and bioavailability. In addition, benzofurans are found in a significant number of natural products. Many natural benzofurans have physiological, pharmacological, and toxic effects [61]. Compound 4e is already known for its osteogenic activity [30]. Excess glucocorticoid is associated with increased bone marrow fat [41, 62]. Compound 4e showed its osteoblast rescuing effect against palmitate induced osteoblast death [31] thus suggesting that compound 4e modulates the bone marrow environment in favor of bone formation.

Conclusion

In conclusion, our results provide both in vitro and in vivo proof of the influence of compound 4e on the preservation of bone loss against glucocorticoid induced osteoporosis by modulating Wnt signaling. It can be a promising molecule to treat GIOP by maintaining osteoblast homeostasis.

Acknowledgements The authors would like to acknowledge Achchhelal Vishwakarma for Annexin/PI apoptosis assay. We also acknowledge Geet K. Nagar for wax tissue preparation and Hematoxylin & Eosin staining and Rima Ray Sarkar for confocal microscopy for RUNX2 immunocytochemistry. CSIR-CDRI communication number for this manuscript is 10350.

Author contributions Study conception and design: AKT, DR, PK, PK, KVS, RT Methodology: AKT, DR, PK, PK Acquisition of data: AKT, DR, PK, PK Analysis and interpretation of data: AKT, DR, PK, KVS, RT Drafting of the manuscript: AKT, DR, PK, KVS, RT.

Funding This work was supported by grants and fellowship from the Council of Scientific and Industrial Research (CSIR), University Grant Commission (UGC), and Indian Council of Medical Research (ICMR) New Delhi, India.

Data availability The data generated during the current study are available from the corresponding author on reasonable request.

Declarations

Conflict of interest The authors declare that they have no known competing financial interests.

References

1. Oray M, Abu Samra K, Ebrahimiadib N et al (2016) Long-term side effects of glucocorticoids. Expert Opin Drug Saf 15:457–465
2. Overman RA, Yeh JY, Deal CL (2013) Prevalence of oral glucocorticoid usage in the United States: a general population perspective. Arthritis Care Res 65:294–298. https://doi.org/10.1002/acr.21796
3. Walsh LJ, Wong CA, Pringle M, Tattersfield AE (1996) Use of oral corticosteroids in the community and the prevention of secondary osteoporosis: a cross sectional study. Br Med J 313:344–346. https://doi.org/10.1136/bmj.313.7053.344
4. Ledford H (2020) Coronavirus breakthrough: dexamethasone is first drug shown to save lives. Nature 582:469. https://doi.org/10.1038/D41586-020-01824-5
5. Adami G, Saag KG (2019) Glucocorticoid-induced osteoporosis: 2019 concise clinical review. Osteoporos Int 30:1145–1156
6. Gudbjornsson B, Juliusson UI, Gudjonsson FV (2002) Prevalence of long term steroid treatment and the frequency of decision making to prevent steroid induced osteoporosis in daily clinical practice. Ann Rheum Dis 61:32–36. https://doi.org/10.1136/ard.61.1.32
7. Hofbauer LC, Gori F, Riggs BL et al (1999) Stimulation of osteoprotegerin ligand and inhibition of osteoprotegerin production by glucocorticoids in human osteoblastic lineage cells: potential paracrine mechanisms of glucocorticoid-induced osteoporosis. Endocrinology 140:4382–4389. https://doi.org/10.1210/endo.140.10.7034
8. Kondo T, Kitazawa R, Yamaguchi A, Kitazawa S (2008) Dexamethasone promotes osteoclastogenesis by inhibiting osteoprotegerin through multiple levels. J Cell Biochem 103:335–345. https://doi.org/10.1002/jcb.21414
9. Beier EE, Sheu TJ, Resseguie EA et al (2017) Sclerostin activity plays a key role in the negative effect of glucocorticoid signaling on osteoblast function in mice. Bone Res. https://doi.org/10.1038/BONERES.2017.13
10. Hayashi K, Yamaguchi T, Yano S et al (2009) BMP/Wnt antagonists are upregulated by dexamethasone in osteoblasts and reversed by alendronate and PTH: potential therapeutic targets for glucocorticoid-induced osteoporosis. Biochem Biophys Res Commun 379:261–266. https://doi.org/10.1016/j.bbrc.2008.12.035
11. Yao W, Cheng Z, Busse C et al (2008) Glucocorticoid excess in mice results in early activation of osteoclastogenesis and adipogenesis and prolonged suppression of osteogenesis: a longitudinal study of gene expression in bone tissue from glucocorticoid-treated mice. Arthritis Rheum 58:1674–1686. https://doi.org/10.1002/art.23454
12. Sui B, Hu C, Liao L, Chen Y, Zhang X, Fu X, Zheng C, Li M, Wu L, Zhao X, Jin Y (2016) Mesenchymal progenitors in osteopenias of diverse pathologies: differential characteristics in the common shift from osteoblastogenesis to adipogenesis. Sci Rep. https://doi.org/10.1038/SREP30186
13. Zhou H, Mak W, Zheng Y et al (2008) Osteoblasts directly control lineage commitment of mesenchymal progenitor cells through Wnt signaling. J Biol Chem 283:1936–1945. https://doi.org/10.1074/jbc.M702687200
14. Xing Ming S, Blair HC, Yang X et al (2000) Tandem repeat of C/EBP binding sites mediates PPARγ2 gene transcription in glucocorticoid-induced adipocyte differentiation. J Cell Biochem 76:518–527. https://doi.org/10.1002/(SICI)1097-4644(20000301)76:3%3c518::AID-JCB18%3e3.0.CO;2-M
15. Komori T (2016) Glucocorticoid signaling and bone biology. Horm Metab Res 48:755–763. https://doi.org/10.1055/S-0042-110571
16. Almeida M, Han L, Ambrogini E et al (2011) Glucocorticoids and tumor necrosis factor α increase oxidative stress and suppress Wnt protein signaling in osteoblasts. J Biol Chem 286:44326–44335. https://doi.org/10.1074/jbc.M111.283481
17. Khan AA, Morrison A, Hanley DA et al (2015) Diagnosis and management of osteonecrosis of the jaw: a systematic review and international consensus. J Bone Miner Res 30:3–23
18. Koh JH, Myong JP, Yoo J et al (2017) Predisposing factors associated with atypical femur fracture among postmenopausal Korean women receiving bisphosphonate therapy: 8 years' experience in a single center. Osteoporos Int 28:3251–3259. https://doi.org/10.1007/s00198-017-4169-y

19. Saag KG, Wagman RB, Geusens P et al (2018) Denosumab versus risedronate in glucocorticoid-induced osteoporosis: a multicentre, randomised, double-blind, active-controlled, double-dummy, non-inferiority study. Lancet Diabetes Endocrinol 6:445–454. https://doi.org/10.1016/S2213-8587(18)30075-5
20. Anastasilakis AD, Polyzos SA, Makras P et al (2017) Clinical features of 24 patients with rebound-associated vertebral fractures after denosumab discontinuation: systematic review and additional cases. J Bone Miner Res 32:1291–1296. https://doi.org/10.1002/jbmr.3110
21. Cottineau B, Toto P, Marot C et al (2002) Synthesis and hypoglycemic evaluation of substituted pyrazole-4-carboxylic acids. Bioorganic Med Chem Lett 12:2105–2108. https://doi.org/10.1016/S0960-894X(02)00380-3
22. Thévenin M, Thoret S, Grellier P, Dubois J (2013) Synthesis of polysubstituted benzofuran derivatives as novel inhibitors of parasitic growth. Bioorganic Med Chem 21:4885–4892. https://doi.org/10.1016/j.bmc.2013.07.002
23. Koca M, Servi S, Kirilmis C et al (2005) Synthesis and antimicrobial activity of some novel derivatives of benzofuran: Part 1. Synthesis and antimicrobial activity of (benzofuran-2-yl)(3- phenyl-3-methylcyclobutyl) ketoxime derivatives. Eur J Med Chem 40:1351–1358. https://doi.org/10.1016/j.ejmech.2005.07.004
24. Xie F, Zhu H, Zhang H et al (2015) In vitro and in vivo characterization of a benzofuran derivative, a potential anticancer agent, as a novel Aurora B kinase inhibitor. Eur J Med Chem 89:310–319. https://doi.org/10.1016/j.ejmech.2014.10.044
25. Kumar S, Dare L, Vasko-Moser JA et al (2007) A highly potent inhibitor of cathepsin K (relacatib) reduces biomarkers of bone resorption both in vitro and in an acute model of elevated bone turnover in vivo in monkeys. Bone 40:122–131. https://doi.org/10.1016/j.bone.2006.07.015
26. Modukuri RK, Choudhary D, Gupta S et al (2017) Benzofuran-dihydropyridine hybrids: a new class of potential bone anabolic agents. Bioorganic Med Chem 25:6450–6466. https://doi.org/10.1016/j.bmc.2017.10.018
27. Tang CH, Sen YR, Chien MY et al (2008) Enhancement of bone morphogenetic protein-2 expression and bone formation by coumarin derivatives via p38 and ERK-dependent pathway in osteoblasts. Eur J Pharmacol 579:40–49. https://doi.org/10.1016/j.ejphar.2007.10.013
28. Gupta A, Ahmad I, Kureel J et al (2016) Differentiation of skeletal osteogenic progenitor cells to osteoblasts with 3,4-diarylbenzopyran based amide derivatives: novel osteogenic agents. Eur J Med Chem 121:82–99. https://doi.org/10.1016/j.ejmech.2016.05.023
29. Woo JT, Kawatani M, Kato M et al (2006) Reveromycin A, an agent for osteoporosis, inhibits bone resorption by inducing apoptosis specifically in osteoclasts. Proc Natl Acad Sci USA 103:4729–4734. https://doi.org/10.1073/pnas.0505663103
30. Kushwaha P, Tripathi AK, Gupta S et al (2018) Synthesis and study of benzofuran-pyran analogs as BMP-2 targeted osteogenic agents. Eur J Med Chem 156:103–117. https://doi.org/10.1016/j.ejmech.2018.06.062
31. Tripathi AK, Rai D, Kothari P et al (2020) Benzofuran pyran compound rescues rat and human osteoblast from lipotoxic effect of palmitate by inhibiting lipid biosynthesis and promoting stabilization of RUNX2. Toxicol Vitr. https://doi.org/10.1016/j.tiv.2020.104872
32. Sashidhara KV, Kumar M, Khedgikar V et al (2013) Discovery of coumarin-dihydropyridine hybrids as bone anabolic agents. J Med Chem 56:109–122. https://doi.org/10.1021/jm301281e
33. Kothari P, Sinha S, Sardar A et al (2020) Inhibition of cartilage degeneration and subchondral bone deterioration by: *Spinacia oleracea* in human mimic of ACLT-induced osteoarthritis. Food Funct 11:8273–8285. https://doi.org/10.1039/d0fo01125h
34. Kushwaha P, Khedgikar V, Gautam J et al (2014) A novel therapeutic approach with Caviunin-based isoflavonoid that en routes bone marrow cells to bone formation via BMP2/Wnt-β-catenin signaling. Cell Death Dis. https://doi.org/10.1038/cddis.2014.350
35. Nie Z, Deng S, Zhang L et al (2019) Crocin protects against dexamethasone-induced osteoblast apoptosis by inhibiting the ROS/Ca2+-mediated mitochondrial pathway. Mol Med Rep 20:401–408. https://doi.org/10.3892/mmr.2019.10267
36. Xie B, Wu J, Li Y et al (2019) Geniposide alleviates glucocorticoid-induced inhibition of osteogenic differentiation in MC3T3-E1 cells by ERK pathway. Front Pharmacol. https://doi.org/10.3389/fphar.2019.00411
37. Karvande A, Khan S, Khan I et al (2018) Discovery of a tetrazolyl β-carboline with in vitro and in vivo osteoprotective activity under estrogen-deficient conditions. Medchemcomm 9:1213–1225. https://doi.org/10.1039/c8md00109j
38. Karvande A, Kushwaha P, Ahmad N et al (2018) Glucose dependent miR-451a expression contributes to parathyroid hormone mediated osteoblast differentiation. Bone 117:98–115. https://doi.org/10.1016/j.bone.2018.09.007
39. Ahmad N, Kushwaha P, Karvande A et al (2019) MicroRNA-672-5p Identified during weaning reverses osteopenia and sarcopenia in ovariectomized mice. Mol Ther - Nucleic Acids 14:536–549. https://doi.org/10.1016/j.omtn.2019.01.002
40. Pal S, Mittapelly N, Husain A et al (2020) A butanolic fraction from the standardized stem extract of *Cassia occidentalis* L delivered by a self-emulsifying drug delivery system protects rats from glucocorticoid-induced osteopenia and muscle atrophy. Sci Rep. https://doi.org/10.1038/s41598-019-56853-6
41. Li J, Zhang N, Huang X et al (2013) Dexamethasone shifts bone marrow stromal cells from osteoblasts to adipocytes by C/EBPαlpha promoter methylation. Cell Death Dis. https://doi.org/10.1038/cddis.2013.348
42. Adhikary S, Choudhary D, Tripathi AK et al (2019) FGF-2 targets sclerostin in bone and myostatin in skeletal muscle to mitigate the deleterious effects of glucocorticoid on musculoskeletal degradation. Life Sci 229:261–276. https://doi.org/10.1016/j.lfs.2019.05.022
43. O'Brien CA, Jia D, Plotkin LI et al (2004) Glucocorticoids act directly on osteoblasts and osteocytes to induce their apoptosis and reduce bone formation and strength. Endocrinology 145:1835–1841. https://doi.org/10.1210/en.2003-0990
44. Il YS, Yoon HY, Jeong SY, Chung YS (2009) Glucocorticoid induces apoptosis of osteoblast cells through the activation of glycogen synthase kinase 3β. J Bone Miner Metab 27:140–148. https://doi.org/10.1007/s00774-008-0019-5
45. Ko FC, Van Vliet M, Ellman R et al (2017) Treatment with a soluble bone morphogenetic protein type 1A receptor (BMPR1A) fusion protein increases bone mass and bone formation in mice subjected to hindlimb unloading. JBMR plus 1:66–72. https://doi.org/10.1002/jbm4.10012
46. Hu J, Mao Z, He S et al (2017) Icariin protects against glucocorticoid induced osteoporosis, increases the expression of the bone enhancer DEC1 and modulates the PI3K/Akt/GSK3β/β-catenin integrated signaling pathway. Biochem Pharmacol 136:109–121. https://doi.org/10.1016/j.bcp.2017.04.010
47. Piemontese M, Xiong J, Fujiwara Y et al (2016) Cortical bone loss caused by glucocorticoid excess requires RANKL production by osteocytes and is associated with reduced OPG expression in mice. Am J Physiol - Endocrinol Metab 311:E587–E593. https://doi.org/10.1152/ajpendo.00219.2016
48. Ohlsson C, Nilsson KH, Henning P et al (2018) WNT16 overexpression partly protects against glucocorticoid-induced bone loss. Am J Physiol Endocrinol Metab 314:E597–E604. https://doi.org/10.1152/ajpendo.00292.2017

49. Zhong Z, Zylstra-Diegel CR, Schumacher CA et al (2012) Wntless functions in mature osteoblasts to regulate bone mass. Proc Natl Acad Sci USA. https://doi.org/10.1073/pnas.1120407109
50. Ohnaka K, Tanabe M, Kawate H et al (2005) Glucocorticoid suppresses the canonical Wnt signal in cultured human osteoblasts. Biochem Biophys Res Commun 329:177–181. https://doi.org/10.1016/j.bbrc.2005.01.117
51. Sato AY, Cregor M, Delgado-Calle J et al (2016) protection from glucocorticoid-induced osteoporosis by anti-catabolic signaling in the absence of Sost/Sclerostin. J Bone Miner Res 31:1791–1802. https://doi.org/10.1002/jbmr.2869
52. Recombinant human osteogenic protein-1 (hOP-1) induces new bone formation in vivo with a specific activity comparable with natural bovine osteogenic protein and stimulates osteoblast proliferation and differentiation in vitro - PubMed. https://pubmed.ncbi.nlm.nih.gov/1328198/. Accessed 20 Nov 2020
53. Urist MR (1965) Bone: Formation by autoinduction. Science 150:893–899. https://doi.org/10.1126/science.150.3698.893
54. Wozney JM, Rosen V, Celeste AJ et al (1988) Novel regulators of bone formation: molecular clones and activities. Science 242:1528–1534. https://doi.org/10.1126/science.3201241
55. Luppen CA, Smith E, Spevak L et al (2003) Bone morphogenetic protein-2 restores mineralization in glucocorticoid-inhibited MC3T3-E1 osteoblast cultures. J Bone Miner Res 18:1186–1197. https://doi.org/10.1359/jbmr.2003.18.7.1186
56. Luppen CA, Chandler RL, Noh T et al (2008) BMP-2 vs. BMP-4 expression and activity in glucocorticoid-arrested MC3T3-E1 osteoblasts: Smad signaling, not alkaline phosphatase activity, predicts rescue of mineralization. Growth Factors 26:226–237. https://doi.org/10.1080/08977190802277880
57. Pereira RC, Delany AM, Canalis E (2002) Effects of cortisol and bone morphogenetic protein-2 on stromal cell differentiation: correlation with CCAAT-enhancer binding protein expression. Bone 30:685–691. https://doi.org/10.1016/S8756-3282(02)00687-7
58. Chen Z, Xue J, Shen T et al (2016) Curcumin alleviates glucocorticoid-induced osteoporosis through the regulation of the Wnt signaling pathway. Int J Mol Med 37:329–338. https://doi.org/10.3892/ijmm.2015.2432
59. Gordon EM, Barrett RW, Dower WJ et al (1994) Applications of combinatorial technologies to drug discovery. 2. Combinatorial organic synthesis, library screening strategies, and future directions. J Med Chem 37:1385–1401. https://doi.org/10.1021/jm00036a001
60. McGrath NA, Brichacek M, Njardarson JT (2010) A graphical journey of innovative organic architectures that have improved our lives. J Chem Educ 87:1348–1349
61. Kao CL, Chern JW (2001) A convenient synthesis of naturally occurring benzofuran ailanthoidol. Tetrahedron Lett 42:1111–1113. https://doi.org/10.1016/S0040-4039(00)02163-8
62. Ferraù F, Giovinazzo S, Messina E et al (2020) High bone marrow fat in patients with Cushing's syndrome and vertebral fractures. Endocrine 67:172–179. https://doi.org/10.1007/s12020-019-02034-4